



Relative environmental stability in the Hula Valley (northern Israel) during the last glacial-interglacial transition

Elizabeth Bunin ^{a,*} , Gonen Sharon ^b, Birgit Schröder ^c, Steffen Mischke ^a

^a Institute of Earth Sciences, University of Iceland, Sturlugata 7, 102, Reykjavík, Iceland

^b MA Program in Galilee Studies, Tel Hai College, 1220800, Upper Galilee, Israel

^c GFZ Helmholtz Centre for Geosciences, Telegrafenberg, 14473, Potsdam, Germany

ARTICLE INFO

Handling editor: Dr Donatella Magri

Keywords:

Levant
Epipaleolithic
LGM
Quaternary
Ostracoda
Geochemistry
Sedimentology
Paleolimnology

ABSTRACT

This study presents the first multidecadal-resolution, carbonate stable isotope record from Paleolake Hula, a hydrologically-open freshwater lake located along the Dead Sea Transform in northern Israel. This lake was an important landscape feature to prehistoric hunter-fisher-gatherer societies since at least the early Middle Pleistocene, and some of the Levant's most important archeological sites are located along its paleoshorelines. The lacustrine sedimentary sequence studied here is the first known from the southern Levant to preserve both a continuous record of regional environmental conditions as well as artifacts attributed to cultures from all three stages of the Epipaleolithic period: the Early Epipaleolithic Masraqan, the Middle Epipaleolithic Geometric Kebaran and the Late/Terminal Epipaleolithic Natufian. While the Epipaleolithic was a time of dramatic cultural change in this region, and the transition from the last glacial to the present (Holocene) interglacial brought with it a dramatic reorganization of global climate systems, our record shows that environmental conditions in the Hula Valley were mild, stable, and continuously favorable for human habitation. Here average ostracod carbonate $\delta^{18}\text{O}$ and $\delta^{13}\text{C}$ values measured exhibit variation within a narrow range (c. 3 %) and show no evidence for extreme temperatures or aridity. High intra-sample variability of the dataset indicates that short-term (day-to-week scale) variability in the water isotopic composition and temperature was significant. This is especially pronounced during times of lower lake volume, when thermal and isotopic buffering capacity were reduced. The multidecadal resolution of this sedimentary sequence allows for the identification of centennial-scale climate developments previously poorly known from the eastern Mediterranean region, including evidence for a two-phase Younger Dryas. Although shifts in the local hydroclimate are recognizable in the proxy datasets, their real-world expressions are expected to have been modest, and unlikely to have significantly impacted the valley's terrestrial biota. Results confirm the importance of both the eastern Mediterranean Sea as the primary moisture source for precipitation and the contribution of northern moisture sources to the water balance of downstream lakes. The results also highlight the complexity of interpreting carbonate stable isotope records from hydrologically-open lakes and the importance of viewing them in conjunction with other proxies such as grain size, geochemical, lithological and micropaleontological data.

1. Introduction

At the end of most recent glacial period (c. 22 to 12 cal ka BP), global climate experienced a series of dramatic, millennial-scale climatic fluctuations in which conditions alternated between stadial (cooler) and interstadial (milder) environments against the backdrop of gradually warming long-term average temperatures following the Last Glacial Maximum (LGM) (Dansgaard et al., 1982; Johnsen et al., 1992; Denton et al., 2010; Clark et al., 2012; Menviel et al., 2011; Buizert et al., 2018;

Barker and Knorr, 2021). While the effects of these events may be most extreme, and their signatures most visible, near the poles, their impacts are also visible in low- and mid-latitude areas far beyond the limits of terrestrial ice sheets (Naughton et al., 2009; Clark et al., 2012; Landais et al., 2018; Huang et al., 2019; Camuera et al., 2021; Vadsaria et al., 2022). In the climatically sensitive southern Levant-eastern Mediterranean region, even small changes in temperature, normalized humidity, precipitation, seasonality and atmospheric moisture can have noticeable effects on regional hydroclimate and local environments (Goodfriend

* Corresponding author.

E-mail address: ejb6@hi.is (E. Bunin).

and Magaritz, 1988; Milano et al., 2012; Goldsmith et al., 2017). For this reason, high-resolution, well-dated environmental records from the Levant are essential to understand the various components of the hydrological cycle and their impact on the region's overall water balance. This is a necessary step in contextualizing the cultural developments of the terminal Pleistocene, which include significant advancements such as the transition from foraging to farming and the emergence of sedentary settlements (Kaufman, 1992; Belfer-Cohen and Bar-Yosef, 2000; Belfer-Cohen and Hovers, 2005; Goring-Morris, 2009; Finlayson and Warren, 2010; Maher et al., 2012; Richter and Maher, 2013; Dubreuil and Nadel, 2015; Abadi and Grosman, 2019; Belfer-Cohen and Goring-Morris, 2020; Macdonald et al., 2018; Valletta and Grosman, 2025).

Our current understanding of late Pleistocene environmental conditions in the Levant is the product of decades of research at dozens of sites using diverse biological, chemical and physical proxies which reflect various components of the regional climatic system (Horowitz, 1973; Gat and Magaritz, 1980; Weinstein-Evron, 1983; Goodfriend and Magaritz, 1988; Baruch and Bottema, 1991; Tchernov 1992; Frumkin et al., 2000; Robinson et al., 2006; Enzel et al., 2008; Roberts et al., 2008; Almogi-Labin et al., 2009; Rambeau, 2010; Miebach et al., 2017, 2019; Goldsmith et al., 2017; Ben-Dor et al., 2021; Tierney et al., 2022; Stein et al., 2025). Here, the use of carbonate stable isotopes to understand variability in hydroclimate has a particularly long and successful history in the eastern Mediterranean region: periods of enhanced water availability, changes in vegetation composition, temperature and precipitation-evaporation balances have all been identified in speleothems from Israeli and Lebanese caves (Bar-Matthews et al., 1996, 2000, 2003; Bar-Matthews and Ayalon, 1997; Vaks et al., 2006, 2007; Cheng et al., 2015). High-resolution studies using gastropod shells have shown seasonal patterns in precipitation and evaporation in northern Israel (Zaaron et al., 2016; Rice et al., 2023). Sea surface temperatures, sea level changes and circulation patterns have all been reconstructed using the isotopic compositions of planktonic foraminiferal tests from eastern Mediterranean sediment cores (Fig. 1; Grant et al., 2012; Hennekam et al., 2014; Cornuault et al., 2016; Le Houedec et al., 2020). These records of eastern Mediterranean surface water chemistry have also been used to isolate and remove the source water signal from

speleothem carbonate oxygen isotope records in caves and lakes where direct evaporation-precipitation links are established (Almogi-Labin et al., 2009; Develle et al., 2010; Grant et al., 2016; Bar-Matthews et al., 2019).

During the LGM, locally-high water levels are reconstructed for Lakes Lisan and Hula and attributed to large volumes of freshwater input (Stein et al., 1997; Bartov et al., 2003; Hazan et al., 2005; Torfstein et al., 2015; Miebach et al., 2017; Bunin et al., 2024). Increased precipitation is not, however, reflected in pollen-based vegetation reconstructions for this region, in the stable isotope records of local speleothems or in marine records from the eastern Mediterranean Sea (Fig. 1; Bar-Matthews et al., 2003; Langgut et al., 2011; Grant et al., 2016; Chen and Litt, 2018; Miebach et al., 2019). Furthermore, modelling studies confirm that both high lake levels and the expansion of mesic habitats are possible under lower precipitation conditions, especially when evaporation is significantly suppressed (Bartov et al., 2003; Hazan et al., 2005; Torfstein et al., 2015; Miebach et al., 2017, 2019; Langgut et al., 2021; Ludwig and Hochman, 2022; Bunin et al., 2024). Shifts in the seasonal distribution of precipitation and changes in flood frequency may have also led to high effective moisture without increasing the total amount of precipitation falling annually (Enzel et al., 2008; Ben Dor et al., 2021). According to Goldsmith et al. (2017), two scenarios proposed to explain the hydrological regime of the LGM in this region necessitate either increased or decreased normalized humidity (relative to the present) with either heavier rainfall events or an increase in the number of annual rainfall events, respectively; in the event of higher annual precipitation, moisture trajectories over the Mediterranean were likely shifted southward (Goldsmith et al., 2017).

The late glacial period and last glacial-interglacial transition (c. 18–11.7 cal ka BP) was a time of dramatic environmental changes as the global climate shifted between stadial (Heinrich Stadial 1; Younger Dryas Stadial) and interstadial (Bølling-Allerød) states (Dansgaard et al., 1982; Johnsen et al., 1992; Denton et al., 2010; Menviel et al., 2011; Buizert et al., 2018; Barker and Knorr, 2021). Signals of these changes are seen in paleoenvironmental archives from all over the world, however, in the Mediterranean zone of the Levant, few continuous paleoenvironmental archives exist at the resolution necessary to study how these changes are expressed at the local and regional scale (Roberts

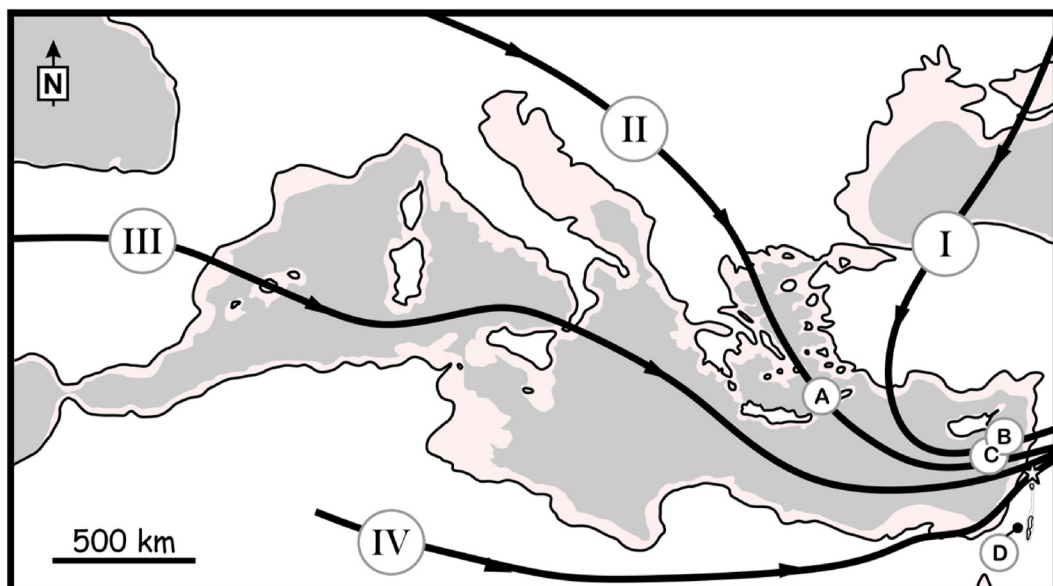


Fig. 1. The Mediterranean Sea showing locations mentioned in the study: Aegean Sea sediment core LC-21 (A; Grant et al., 2012, 2016), Levantine Basin sediment cores MD95-9501 (B; Almogi-Labin et al., 2009) and MD84-632 (C; Essallami et al., 2007), Soreq Cave (D; Bar-Matthews et al., 2003) and the Hula Valley (star). The modern Mediterranean Sea coastline is shown in black. Additional area exposed subaerially during the LGM, when relative sea levels were estimated to be approximately 100 m lower, is shown shaded in light grey (Thiede, 1978). The air mass trajectories shown (thick black lines with arrows) are those initially described by Gagin and Neumann (1974) but are labeled using the numbering scheme of Rindberger et al. (1990).

et al., 2008). One suitable record is the sedimentary sequence exposed at the Jordan River Dureijat (JRD) site, where fine-grained sediment accumulation occurred continuously in a shallow lacustrine environment from c. 21.1 to c. 11.3 cal ka BP at a rate of approximately 20–40 cm ka⁻¹ (Figs. 2 and 3; Sharon et al., 2020; Bunin et al., 2024).

The aim of our study is to use ostracod valves from the JRD sedimentary sequence to produce the first multidecadal-resolution, continuous stable isotope record of late glacial conditions in northern Israel, motivated by a need to better understand water availability in the late Pleistocene Hula Valley and the causes of water level change in the lakes located along the Dead Sea Transform. To this end, we investigate which factors control Paleolake Hula's isotopic composition and how changes in carbonate δ¹⁸O and δ¹³C values and δ¹⁸O-δ¹³C covariance reflect changes in the lake, catchment, and regional environment systems. This newly produced record of hydroclimate change in the Hula Valley is then used to refine our understanding of the environmental circumstances surrounding the transitions from the Early to Middle and Middle to Late phases of the Epipaleolithic in the southern Levant.

2. Study area

2.1. The Hula valley

The Hula Valley is a flat-bottomed, rhomb-shaped pull-apart basin located along the Dead Sea Transform fault system (Fig. 2; Heimann and Ron, 1987; Weinberger et al., 2009). The floor of the Hula Valley has an area of approximately 150 km² and lies at an elevation of approximately 70 m above sea level (masl). The valley is bordered by the limestone Naftali Mountains to the west, the basaltic Golan Plateau to the east and the Korazim block to the south (Fleischer, 1968; Horowitz, 1973; Heimann, 1990; Belitzky, 2002; Heimann et al., 2009). North of the Hula Valley lies the Lebanon restraining bend: here, the fault system splay into multiple active fault segments, the largest of which is the Yam-mouneh fault (Weinberger et al., 2009). The northern margin of the Hula Basin is poorly defined, but in the northeast abuts the Hermon Range and Anti-Lebanon Mountains. The catchment covers a total area of 1470 km².

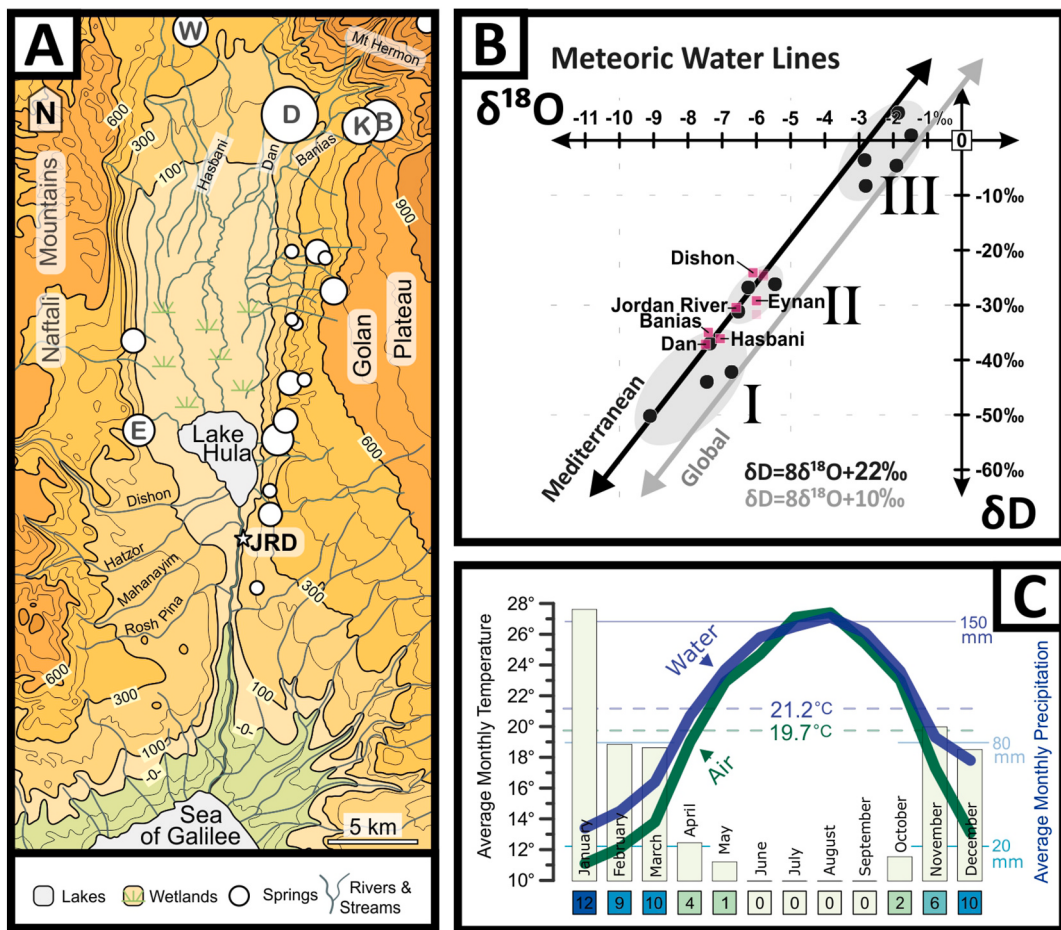


Fig. 2. A) The Hula Valley and location of JRD excavation (star). White circles indicate springs, with size of the circles being proportional to their annual discharge after Babad et al. (2019). The five largest springs are labeled as follows: Wazzani (W), Eynan (E), Dan (D), Ktznim (K) and Banias (B). Base map is redrawn after Survey of Israel (1951). Scale is 1:250,000, contour interval is 100 m. Lake surface elevation for the Sea of Galilee (212 mbsl) reflects the mean water level for 1937; surface level shown for Lake Hula is 68 masl and was measured in 1951. B) Water isotope values for modern precipitation (black circles; Rindberger et al. 1983), river water (pink squares; Gat and Dansgaard 1972) and springs (pink squares; Gat and Dansgaard 1972; Babad et al. 2019) plotted relative to the global (grey; Craig, 1961) and local (black; Gat and Carmi 1970) meteoric water lines. Roman numerals refer to moisture sources and pathways shown in Fig. 1. C) Climograph shows average conditions in the Hula Valley prior to the drainage of the lake. Average monthly air temperatures (green line) measured at Yesud Ha Ma'ala for the years 1938–1945 and published in Neumann (1953). Average monthly lake surface water temperatures (blue line) measured for the same time period from the shallow, shore-proximal lake environment near Yesud Ha Ma'ala and originally published in Ashbel (1945). Average monthly precipitation data (1938–1945) from the Ayelet Ha Shahar weather station downloaded from the Israeli Meteorological Service (2025). Shaded boxes along the x-axis show the average number of rainy days per month for the time period 1938–1945 (https://ims.gov.il/en/data_gov). Dashed lines indicate the average annual air (19.7°C; green) and water (21.2°C; blue) temperatures. (For interpretation of the references to colour in this figure legend, the reader is referred to the Web version of this article.)

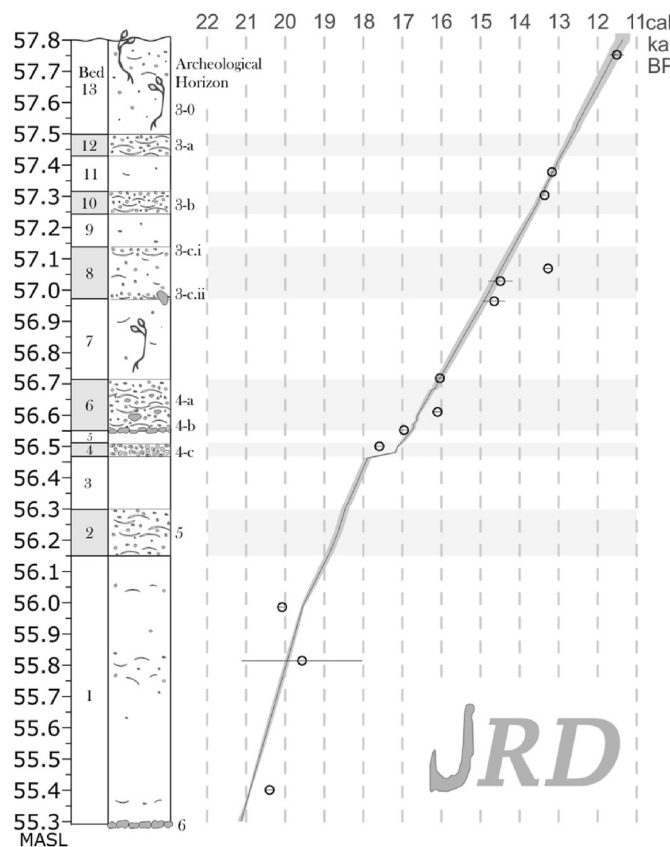


Fig. 3. Stratigraphy and chronology of the Jordan River Dureijat sedimentary sequence. Hollow circles denote the calibrated, unmodelled radiocarbon ages used in the production of the model, which was created using a Poisson sequence in OxCal version 4.4 (Bronk Ramsey, 2008; Reimer et al., 2020). Full details of the radiocarbon dates included and the model's parameters are published in Bunin et al. (2024). The complete set of modelled ages for the Jordan River Dureijat sedimentary sequence is published in Bunin et al. (2023).

2.2. The (hydro)climate of northern Israel

The present-day climate of northern Israel comprises hot and dry summers and cooler winters with precipitation primarily falling during the winter months (Fig. 2; https://ims.gov.il/en/data_gov). This precipitation is primarily associated with the transportation of cold, dry air from the North Atlantic over the Balkans and eastern Mediterranean Sea before entering Israel from the northwest (Fig. 1, trajectory II; Gagin and Neumann, 1974). Evaporated eastern Mediterranean surface water serves as the moisture source for nearly all precipitation falling in northern Israel today (Alpert and Shay-El, 1994; Mariotti, 2010; Seager et al., 2014). In the late Pleistocene, however, Atlantic and/or polar air masses with exclusively or partly continental trajectories may have had larger contributions to regional precipitation (Fig. 1, trajectories I and III; Gat and Carmi, 1987) and, during the LGM, the tracks of storms traveling from the north Atlantic into the Mediterranean may have been shifted south, as proposed in Goldsmith et al. (2017).

Precipitation falling in the surrounding mountains reaches the valley primarily by way of the Jordan River and its tributaries (Goldreich, 2003; Kushnir et al., 2017). Today, this precipitation averages 470 mm per year and falls almost exclusively as rain during the winter months (November through April; ims.gov.il, for the weather station located at Ayelet HaShahar, 3 km west of JRD; Fig. 2), however, precipitation seasonality patterns are shown to have been highly variable throughout the late Pleistocene, and the present pattern of precipitation seasonality was most likely established only recently (Horowitz and Gat, 1984; Langgut et al., 2021; Rice et al., 2023). Additionally, four aquifers

discharge groundwater to the catchment via springs located both along the valley's margins and in the Hermon Range (Fig. 2; Dafny et al., 2006; Babad et al., 2019).

2.3. Lake Hula

The water that collects in the Hula Valley has historically formed a shallow, exorheic freshwater lake ("Lake Hula," also spelled "Lake Huleh") surrounded by peripheral wetlands (Cowgill, 1969; Horowitz, 1973; Dimentman et al., 1992). The lake's one surficial outflow was the Lower Jordan River, which flowed south to the (exorheic) Sea of Galilee and ultimately on to the (endorheic) Dead Sea (Fig. 2). Previously, it was thought that this lake had initially formed approximately thirty thousand years ago with the emplacement of the Yarda Basalt, which was presumed to have dammed the southern Hula Valley and blocked the flow of the Jordan River southward out of the valley (Cowgill, 1969). It is more likely, however, that the lake had already formed by this time, as evidenced by the accumulation of hundreds of meters of lacustrine and wetland sediments representing several glacial-interglacial cycles (Horowitz, 1973; Kafri and Lang, 1987; Rybakov et al., 2003).

Lake Hula existed until 1958, at which time it was drained completely (Dimentman et al., 1992; Hambright and Zohary, 1998; Cohen-Shacham et al., 2011). Today, man-made channels control the flow of the Jordan River across the paleolakebed south to the Sea of Galilee and onward to the Dead Sea. At the time of its drainage, Lake Hula was pear-shaped, with a total surface area of 12–14 km² and with maximum dimensions of 4 km in the East-West direction and approximately 5 km in the North-South direction (Fig. 2; Dimentman et al., 1992). North of the main body of the lake, wetlands are estimated to have covered an additional area of c. 45 km² (Fig. 2; Dimentman et al., 1992). The maximum depth is reported to have fluctuated seasonally, from a summer minimum of c. 1.5 m to a winter maximum of c. 3 m (Hambright and Zohary, 1998). Earlier observations reported slightly larger surface areas and maximum winter water depths up to 5 m (MacGregor, 1870). As such, the historical Lake Hula was shallow and pan-like, with a relative depth of approximately 0.1 % (lake morphometric characteristics given here are reported following the terminology of Wetzel and Likens (2000)). Due to its shallowness, the water column is assumed to have been well-mixed and temperature differences between the surface and bottom water have been described as minimal (Ashbel, 1951; in Neumann, 1953). However, during the warmest months of the year temperature differences may have been as high as 2–3 °C (Jones, 1940). Due to summer insolation and the small thermal capacity of the lake, changes in surface water temperature in excess of 2 °C were observed occurring over the course of an afternoon during one autumn day in 1935 (Washbourne and Jones, 1936).

In modern times, the major inputs of water to the Hula Valley are precipitation, spring-fed streams along the valley's margins, and water from the upper Jordan River and its tributaries: the Hasbani, Dan and Banias rivers. Jordan River water is itself a combination of spring and meteoric water, which falls both as rain and snow, especially in the high-altitude northeast of the catchment (Hermon Range). Highly variable $\delta^{18}\text{O}$ values of precipitation falling in northern Israel (between -12 and $+1\text{ ‰}$; water $\delta^{18}\text{O}$ values here are reported relative to Vienna Standard Mean Ocean Water) were measured during a number of precipitation sampling programs (Gat and Dansgaard, 1972; Rindsberger et al., 1983; Rindsberger et al., 1990). However, the annual weighted average $\delta^{18}\text{O}$ values of modern precipitation closely reflect the origins and trajectories of the air masses as opposed to local temperatures or amount effects (Rindsberger et al., 1990). Modern $\delta^{18}\text{O}$ values of the surrounding aquifers (-7.4 ‰ to -6.1 ‰ ; Babad et al., 2019) and inflowing Jordan River water (estimated to be -6.8 ‰ for the year 1971; Stiller and Hutchinson, 1980) were lower than those of the lake water, likely reflecting evaporation both from the lake surface and along the Jordan (Gat and Dansgaard, 1972; Rindsberger et al., 1990).

2.4. The Jordan River Dureijat archeological site

Epipaleolithic artifacts were first discovered along the banks of the Jordan River during surveys performed prior to dredging operations undertaken to deepen this stretch of the river (Sharon et al., 2002; Marder et al., 2015). As a result, the archeological site of Jordan River Dureijat (JRD) was defined and established, named for its location at the confluence of the Jordan River and Dureijat Stream (Fig. 2). Excavation of the open-air archeological site was carried out annually during the summers 2015–2021. Two archeological units were initially defined, of which the upper (Unit I) is modern and archeologically sterile while the lower (Unit II) is dated to the late Pleistocene (21.1 ± 0.2 to 11.3 ± 0.2 cal ka BP; Fig. 3; Bunin et al., 2024) and contains nine named archeological horizons, initially defined and described in Sharon et al. (2020). Within Unit II, thirteen lithologic beds have been identified and described based on observable changes in the sediments visible at outcrop scale on the exposed walls of the excavation area (Fig. 3; Bunin et al., 2024). Collectively, the sediments of JRD Unit II preserve more than ten thousand years of evidence for changing environmental conditions in and around Paleolake Hula from the LGM to early Holocene (Sharon et al., 2020; Langgut et al., 2021; Bunin et al., 2024). The presence of these lacustrine sediments more than 2 km beyond the 1950s southern limit of Lake Hula implies that the late Pleistocene paleolake was considerably larger than it has been in recent times (Fig. 2).

Sedimentological analyses indicate that sediment accumulation occurred when the site was submerged beneath a shallow column of water, and during times of locally low water level, Epipaleolithic fisher-hunter-gatherers repeatedly returned to this stretch of the lakeshore, leaving behind fishing weights, fishing hooks, stone tools and other artifacts embedded in the silty lake sediments (Sharon et al., 2020; Pedergnana et al., 2021; Rice et al., 2023; Bunin et al., 2024). Stratigraphically, the site preserves seven such low water stands with indications of human presence and six archeologically sterile units deposited during periods of higher water level. During times of high water level human activity was presumably focused in shallower water elsewhere along the lake's paleoshoreline (Bunin et al., 2024). The artifact-bearing layers found at JRD represent all three phases of the Epipaleolithic: the Early Epipaleolithic (Masraqan Cultural Horizon 5), the Middle Epipaleolithic (Geometric Kebaran Cultural Horizons 4a and 4c), and the Late/Final Epipaleolithic (Natufian Cultural Horizons 3a, 3b and 3c; Fig. 3; Sharon et al., 2020). Together, the accumulated artifacts document ten thousand years of human activity, primarily fishing and the collection of other aquatic resources, over the course of the entire Levantine Epipaleolithic (Sharon et al., 2020; Pedergnana et al., 2021). As one of few multiphase Epipaleolithic sites in northern Israel, JRD provides an invaluable record of both significant technological advances and the environmental conditions under which they arose (Sharon et al., 2020; Langgut et al., 2021; Pedergnana et al., 2021).

3. Materials and methods

3.1. Materials

The sediments examined in this study are previously described in earlier JRD publications (Sharon et al., 2020; Bunin et al., 2023, 2024) and were sampled by hand from the East wall of JRD excavation Area B in 2016 (Unit II Lithostratigraphic Beds 1–5) and 2017 (Unit II Beds 5–13; Fig. 3). The exposed sediments were sampled as one continuous vertical profile with a height of 2.5 m and a vertical resolution of 1 cm. Further details on the sampling and photos of the excavation can be found in Bunin et al. (2024), along with all radiocarbon ages available for this site and complete details of the chronostratigraphic modelling. The modelled ages for each sample, together with grain size and geochemical data, are available in the PANGAEA repository (Bunin et al., 2023).

3.2. Initial investigation of the sediments

To determine the amount of ostracod valves found in the JRD sediments, c. 30 g of dry sediments were removed from every eighth sample, treated with 3 % hydrogen peroxide solution overnight, sieved over a 250 μm screen and oven-dried at 60 °C. Ostracod valves present in the sieved fraction greater than 250 μm were counted under 20–40x magnification using a low-power binocular microscope. Only valves more than 50 % complete were counted, with no distinction made between left and right valves. Results are presented normalized to sample weight, as valves per gram dry sediment. Additionally, the presence or absence of ancient foraminifera, lithic clasts and charcoal were noted for each sieved sample.

3.3. Stable isotope analyses

To obtain ostracod valves for the stable isotope analysis, at least 5 g of additional material from each centimeter of the profile was treated and sieved in the same manner as described in section 3.2. Larger sample volumes were prepared from samples expected to contain very few ostracod valves, as determined during the initial counting of valves described above. Under a low-power binocular microscope, valves were identified to genus level and clean and intact *Ilyocypris* spp. valves were removed to glass vials using a metal dissection needle at the University of Iceland, with a preference for large (adult or near-adult) valves. Samples including only fragmented valves or where no *Ilyocypris* spp. valves were present ($n = 18$) were excluded.

From the 214 samples where material was available, 2–6 valves were selected for stable isotope analyses at the Stable Isotope Laboratory of the GFZ Helmholtz Centre for Geosciences in Potsdam. For 52 of these samples, an additional 2–6 valves were analyzed separately to provide information on intra-sample variability. We refer to these pairs of measurements performed on different valves derived from the same sediment samples as duplicate measurements in this text.

To measure the $\delta^{13}\text{C}$ and $\delta^{18}\text{O}$ values of the samples, a MAT 253 isotope ratio mass spectrometer (IRMS) coupled to an automated carbonate device (KIELIV) was used. An amount of carbonate (30–80 μg , corresponding to 2–6 valves) was prepared in vials and reacted with 103 % phosphoric acid at 72 °C for 10 min to produce CO_2 followed by cryogenic purification. The results were calibrated using the international reference material (NBS19) and an internal laboratory reference sample (C1) and are given in delta notation relative to Vienna Pee Dee Belemnite (VPDB). The analytical precision for both the $\delta^{13}\text{C}$ and $\delta^{18}\text{O}$ measurements on reference material is $< 0.07\text{ ‰}$.

To evaluate the degree of $\delta^{18}\text{O}$ - $\delta^{13}\text{C}$ covariance present, the Pearson product moment correlation coefficients (r) were calculated for the entire dataset, for each individual bed, and for each sample including only measurements from the preceding 500 years (r_{500}). Calculation of the r_{500} term was done to show the evolution of the relationship between $\delta^{18}\text{O}$ and $\delta^{13}\text{C}$ values over time.

To examine the degree to which source water $\delta^{18}\text{O}$ variation is expressed in the JRD record we have calculated the difference ($\Delta \delta^{18}\text{O}_{\text{sea-land}}$) between the JRD ostracod carbonate $\delta^{18}\text{O}$ values and same-age foraminiferal $\delta^{18}\text{O}$ measurements from the Levantine Basin sediment core 9501 (Fig. 1; Almogi-Labin et al., 2009), where the Levantine Basin is taken to be broadly representative of the eastern Mediterranean vapor source for precipitation falling over northern Israel today. Levantine Basin $\delta^{18}\text{O}$ values have been resampled to equal-age (40-year) steps using the Past software (version 4.15) as has the JRD record (Hammer et al., 2001). Both records have been corrected for the effects of water temperature change using Equation 1 of Bemis et al. (1998). Temperatures used come from the sea surface temperature record of Essallami et al. (2007), for the Levantine Basin, and the JRD pollen-based temperature modelling of Langgut et al. (2021). Because both records are monospecific, vital effects are not accounted for.

4. Results

4.1. Ostracod, charcoal and lithic clast abundance

Due to the varying thicknesses of the beds, which range from 3 to 28 cm in Beds 2–13 and is 85 cm for Bed 1, between one and four samples were counted from each of Beds 2–13, while 13 samples were counted from Bed 1 (Fig. 4). Ostracod valves belonging to the genera *Ilyocypris* and *Candona* were found in all of the investigated samples, which contain between one and 174 valves per gram dry sediment (Fig. 4). The average (mean) ostracod abundance from all samples ($n = 35$) is 33 valves per gram dry sediment, with a median value of 16 valves per gram. Generally speaking, samples from high water level (odd-numbered) facies contain fewer ostracod valves (average = 28 valves per gram dry sediments, $n = 28$) than samples from lower water level (even-numbered) facies (average = 49, $n = 7$). Sediments deposited in Beds 1–3 (prior to 17.2 cal ka BP) contain on average 42 valves per gram ($n = 18$), whereas sediments in Beds 4–13 (after 17.2 cal ka BP) contain on average 25 valves per gram ($n = 17$). The lowest abundance of ostracod valves is found in Bed 13 (<5 valves per gram). Of the 35 samples investigated, eight include lithic clasts larger than 2 mm, twelve include pieces of charcoal larger than 2 mm, and fourteen include benthic and/or planktonic foraminifera derived from local Cretaceous limestones (Fig. 4).

4.2. Stable isotope analyses

Ostracod valves in good condition were found in 214 of the 232 sediment samples. Including the 52 duplicate measurements, a total of 266 measurements of stable oxygen and carbon isotope compositions were obtained (Supplementary Data A; Fig. 4). Across all samples the average $\delta^{18}\text{O}$ value measured is -4.8 ‰ , with a standard deviation (SD) of 0.9 ‰ . The average $\delta^{13}\text{C}$ value measured is -8.9 ‰ with a SD of 0.8 ‰ . When the duplicate measurements are included, these figures are not significantly different (within 1%; Table 1). For Beds 1–3, the average $\delta^{18}\text{O}$ value is -4.7 ‰ with a SD of 0.7 ‰ and the average $\delta^{13}\text{C}$ value is -9.5 ‰ with a SD of 0.5 ‰ . For Beds 4–13, these values are -4.9 ‰ (SD 1.0%) and -8.3 ‰ (SD 0.6%), respectively. While significant variation is present in both the $\delta^{18}\text{O}$ and $\delta^{13}\text{C}$ records, long-term trends show a 1.0‰ drop in $\delta^{18}\text{O}$ values and a 1.5‰ increase in $\delta^{13}\text{C}$ values over the course of the JRD sequence. Average values for the individual beds vary from -6.0 ‰ to -3.7 ‰ for $\delta^{18}\text{O}$ and from -9.6 ‰ to -8.0 ‰ for $\delta^{13}\text{C}$ values (Table 1). The average $\delta^{13}\text{C}$ value of samples from odd-numbered beds is -9.1 ‰ , compared to -8.5 ‰ for samples from even-numbered beds.

The Pearson correlation coefficient (r) calculated for the entire dataset is 0.06 for all measurements ($r = 0.08$ when the duplicate measurements are excluded). For the individual beds, absolute values are lower in Beds 1–3 than in Beds 4–13 (Table 1). When the Pearson correlation coefficient is calculated only for the preceding 500 years

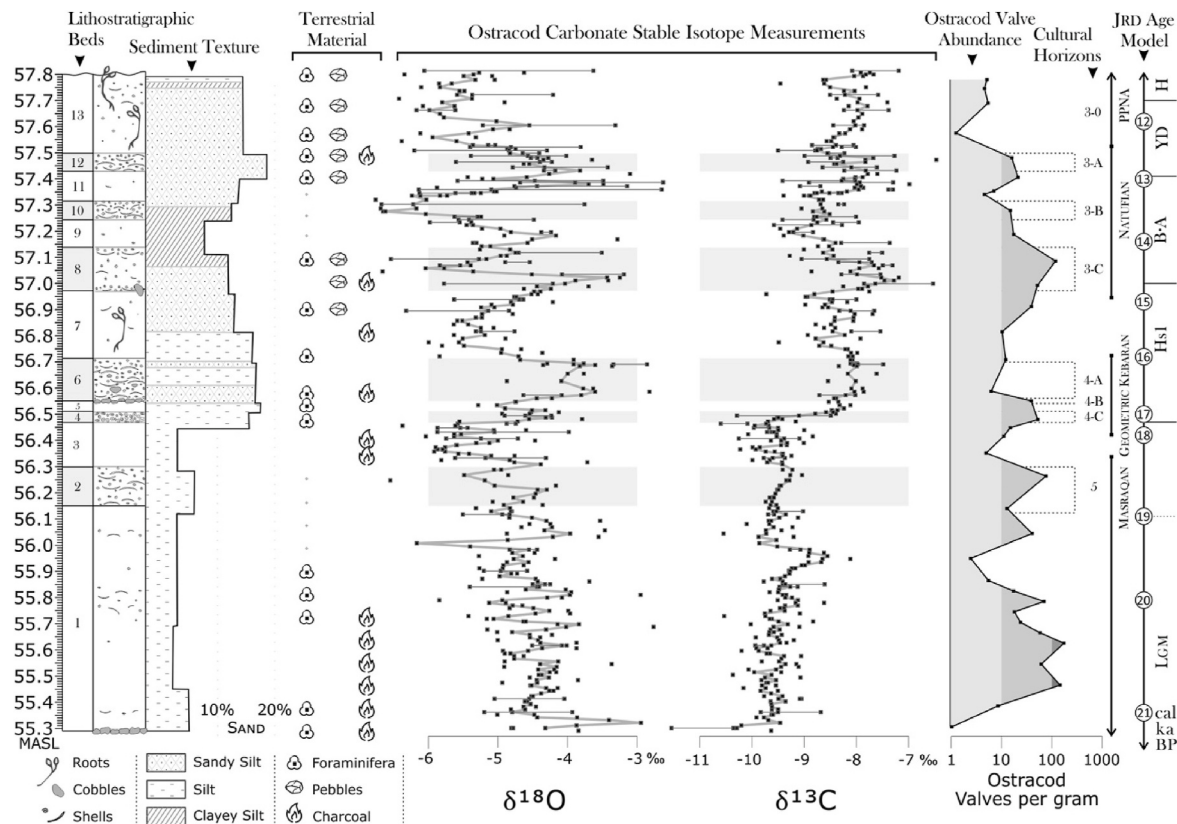


Fig. 4. Sedimentary log of Jordan River Dureijat Unit II showing (from left) the site's lithostratigraphy and an overview of features visible at the outcrop scale, where 'cobbles' refers to all clasts larger than 6 cm (Bunin et al., 2024). Sediment textural descriptions and sand concentrations determined via laser particle size analysis (Bunin et al., 2023, 2024). Presence/absence of foraminifera from Bunin et al. (2024). Presence/absence of charcoal and pebbles (this study) determined under 20–40x microscope magnification during the preparation of the ostracod valves for isotopic analyses; pebbles refers to all fine gravel coarser than 4 mm. Carbon and oxygen isotope measurements for the JRD *Ilyocypris* valves, where black squares indicate individual measurements, horizontal bars between measurements of the same age indicate the spread between the duplicate measurements and grey trend lines present three-point running means (this study). Grey shading in the background of the $\delta^{18}\text{O}$ and $\delta^{13}\text{C}$ results indicates the lithostratigraphic beds as labeled in the log to the left. Abundance of ostracod valves (this study) presented as valves per gram of dry sediment. Cultural horizons and affinities after Sharon et al. (2020). Far right: Y-axis presents the calibrated ages as modelled in Bunin et al. (2023, 2024) vs position in the sequence together with the event stratigraphy of Rasmussen et al. (2014). Abbreviations: PPNA=Pre-Pottery Neolithic A, H=Holocene, YD=Younger Dryas Stadial; B-A=Bølling-Allerød Interstadial, Hsl=Heinrich Stadial 1, LGM=Last Glacial Maximum.

Table 1

Average, standard deviation, minimum and maximum isotope composition measurements, $\delta^{18}\text{O}$ - $\delta^{13}\text{C}$ covariance Pearson correlations coefficients (r) for the stratigraphic beds 1–13, number of measurements per bed and the number of samples investigated per bed (in parentheses). Top values shown are calculated excluding the duplicate measurements. Bottom results are calculated using the average of the duplicate measurements for each sample.

Stratigraphic Bed	Cultural Horizon	Age [cal ka BP]	$\delta^{18}\text{O}_{\text{ave}}$ [%]	$\delta^{18}\text{O}_{\text{sd}}$ [%]	$\delta^{18}\text{O}_{\text{min}}$ [%]	$\delta^{18}\text{O}_{\text{max}}$ [%]	$\delta^{13}\text{C}_{\text{ave}}$ [%]	$\delta^{13}\text{C}_{\text{sd}}$ [%]	$\delta^{13}\text{C}_{\text{min}}$ [%]	$\delta^{13}\text{C}_{\text{max}}$ [%]	Pearson r	Number of measurements (samples investigated)
13	3-0	12.5–11.3	−5.6 −5.5	0.65 0.66	−6.4 −6.4	−4.2 −4.3	−8.2 −8.1	0.45 0.44	−9.5 −9.5	−7.4 −7.4	0.33 0.26	19 (21) 23
12	3-a	12.8–12.5	−4.3 −4.7	0.43 0.43	−5.0 −5.3	−3.7 −3.7	−8.2 −8.3	0.75 0.70	−8.8 −9.1	−6.5 −6.5	0.75 0.91	9 (9) 16
11		13.3–12.8	−4.2 −4.4	1.05 0.77	−5.9 −5.9	−2.6 −3.1	−8.0 −8.0	0.73 0.53	−9.4 −8.9	−7.0 −7.0	0.31 0.27	13 (13) 19
10	3-b	13.5–13.3	−5.7 −5.9	0.95 0.57	−6.8 −6.8	−3.8 −5.2	−8.8 −8.8	0.37 0.37	−9.4 −9.4	−8.2 −8.3	0.66 0.55	7 (7) 9
9		14.1–13.5	−5.1 −5.1	0.88 0.84	−6.6 −6.6	−3.3 −3.3	−8.8 −8.8	0.59 0.50	−9.6 −9.5	−8.0 −7.8	−0.29 −0.22	10 (11) 16
8	3-c	14.8–14.1	−4.8 −4.8	1.08 1.01	−6.7 −6.7	−3.3 −3.3	−8.0 −8.1	0.64 0.67	−9.3 −9.3	−7.2 −7.2	0.37 0.40	14 (14) 20
7		16.0–14.8	−5.1 −5.1	0.58 0.52	−6.3 −6.0	−4.2 −4.2	−8.4 −8.4	0.55 0.54	−9.7 −9.7	−7.5 −7.7	0.26 0.25	22 (22) 25
6	4a + b	16.6–16.0	−3.8 −3.8	0.59 0.61	−4.9 −4.9	−2.8 −2.8	−8.1 −8.0	0.26 0.27	−8.5 −8.5	−7.6 −7.6	0.48 0.57	9 (9) 10
5		16.9–16.6	−4.7 −4.7	0.38 0.41	−5.3 −5.3	−4.2 −4.2	−8.3 −8.4	0.21 0.15	−8.5 −8.5	−8.0 −8.1	−0.38 −0.62	4 (4) 5
4	4-c	17.2–16.9	−4.6 −4.5	0.32 0.27	−4.9 −4.9	−4.1 −4.1	−9.0 −8.9	0.76 0.50	−10.3 −9.5	−8.4 −8.4	0.25 −0.28	5 (6) 6
3		18.4–17.2	−5.2 −5.3	0.77 0.69	−6.4 −6.4	−3.7 −3.7	−9.6 −9.6	0.43 0.40	−10.6 −10.3	−8.8 −8.8	0.06 0.13	21 (21) 26
2	5	19.0–18.4	−4.9 −4.9	0.65 0.65	−6.6 −6.6	−4.2 −4.2	−9.4 −9.5	0.23 0.19	−9.7 −9.7	−9.0 −9.0	−0.08 −0.13	10 (12) 11
1		21.1–19.0	−4.5 −4.5	0.65 0.63	−6.2 −6.2	−2.8 −2.8	−9.5 −9.5	0.50 0.47	−11.5 −11.0	−8.1 −8.1	0.11 0.10	71 (79) 80

(r_{500}), maximum absolute values occur at 15.3 cal ka BP ($r_{500} = 0.86$; Bed 7) and 11.7 cal ka BP ($r_{500} = 0.87$; Bed 13; Fig. 5).

For sediment samples where the isotopic compositions of two aliquots of ostracod valves were measured independently, the duplicate $\delta^{18}\text{O}$ measurements have an average difference of 1.0 ‰ with a SD of 0.8 ‰. For $\delta^{13}\text{C}$ values, the average difference was 0.7 ‰ with a SD of 0.5 ‰. The maximum differences in the measured values were 3.5 ‰ for oxygen and 1.8 ‰ for carbon isotopes. Sets of duplicate measurements from Beds 1–6 generally exhibit smaller differences in both $\delta^{18}\text{O}$ and $\delta^{13}\text{C}$ values than those from Beds 7–13 (Fig. 4).

5. Discussion

5.1. Timing and resolution of the JRD record

The Jordan River Dureijat age model indicates that the ostracod carbonate stable isotope record covers most of the last glacial termination at a multidecadal resolution (Fig. 3; Sharon et al., 2020; Bunin et al., 2023, 2024). It also suggests that very little sediment accumulation

occurred between c. 17.9 ± 0.1 and 17.1 ± 0.1 cal ka BP, indicating that a gap may be present in our stable isotope record corresponding roughly to the contact between Beds 3 and 4. However, no evidence to suggest any sort of unconformity is visible at the outcrop (Bunin et al., 2023, 2024). Instead, we believe it is more likely that a significant change in the sedimentation rate occurred here, as shown in Fig. 3 (Bunin et al., 2023, 2024). In the lower part of the record, prior to 17.9 ± 0.1 cal ka BP, the stable isotope record has a resolution of c. 40 years; after 17.1 ± 0.1 cal ka BP the resolution is c. 50 years (Bunin et al., 2023). The ages of the JRD cultural horizons are therefore broadly consistent with the established timings of the represented cultural entities in the southern Levant (Grosman, 2013; Belfer-Cohen and Goring-Morris, 2020).

5.2. Hydrological connectivity of the late Pleistocene Hula Lake

Earlier stable isotope investigations of Paleolake Hula carbonates indicate that the lake was hydrologically open during the late Pleistocene, with no significant oxygen-carbon isotope covariance occurring in either authigenic carbonates or *Melanopsis* (gastropod) shells deposited

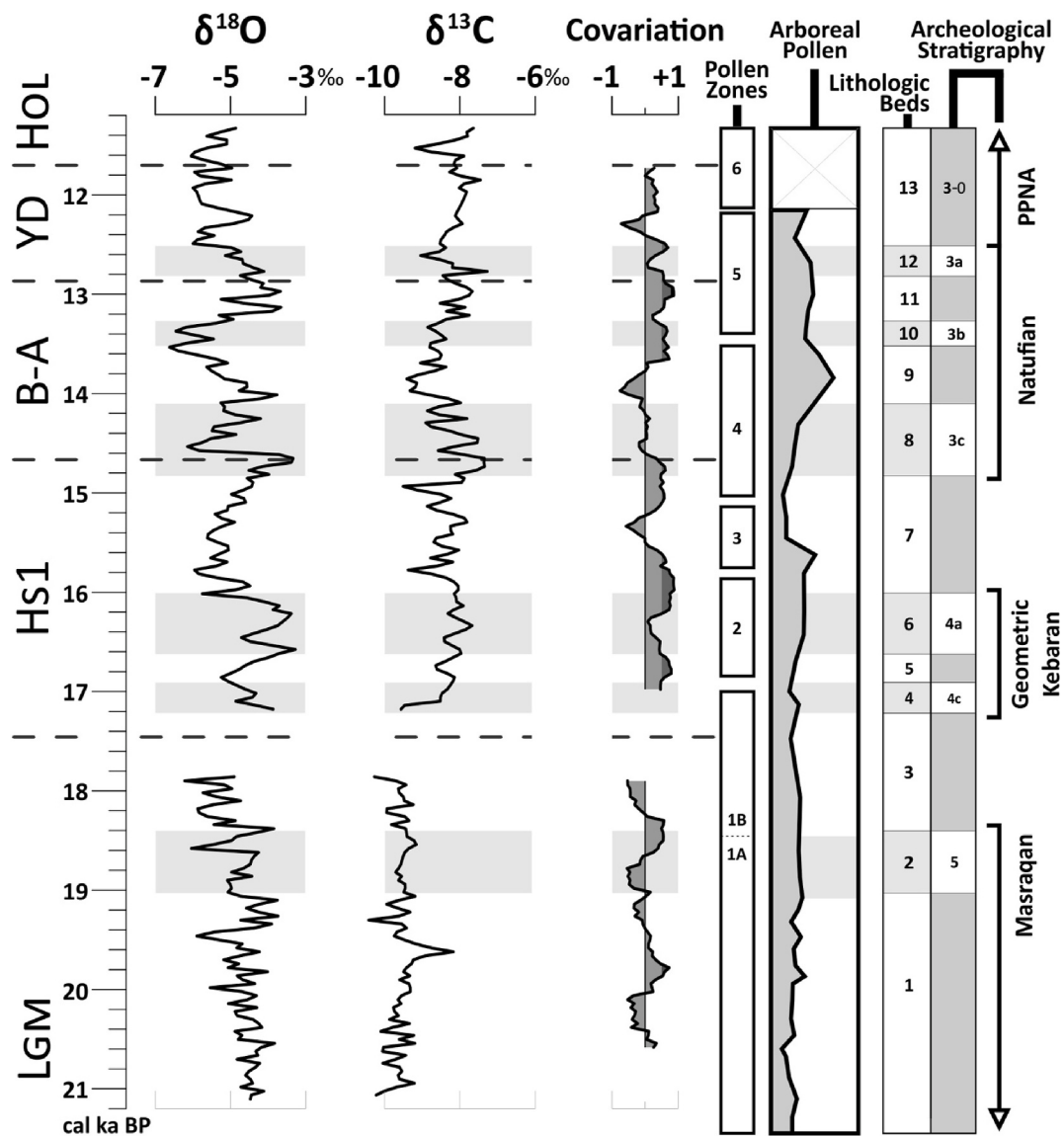


Fig. 5. Jordan River Dureijat ostracod carbonate $\delta^{18}\text{O}$, $\delta^{13}\text{C}$ and $\delta^{18}\text{O}$ - $\delta^{13}\text{C}$ covariation profiles (this study) and pollen zones and arboreal pollen percentages (Langgut et al., 2021). Carbon and oxygen records are resampled to 40-year intervals and smoothed with a three-point Gaussian filter using the software Past (Version 4.15; Hammer et al., 2001). The $\delta^{18}\text{O}$ - $\delta^{13}\text{C}$ covariance values are calculated for the preceding 500 years. All data plotted against the modelled ages published in Bunin et al. (2024). Lithologic beds after Bunin et al. (2024). Archeological stratigraphy and cultural affiliations after Sharon et al. (2020). Event stratigraphy (dashed lines) after Rasmussen et al. (2014). Abbreviations: PPNA=Pre-Pottery Neolithic A, Hol = Holocene, YD=Younger Dryas Stadial; B-A=Bölling-Allerød Interstadial, HS1=Heinrich Stadial 1, LGM = Last Glacial Maximum.

during or since the LGM (Cowgill, 1969; Stiller and Hutchinson, 1980; Rice et al., 2023). Further support for the interpretation of Paleolake Hula as an open lake comes from the JRD ostracod record, which is dominated by freshwater species and where paleoconductivity values, as calculated in Valdimarsson (2017) for the late glacial period, consistently correspond to what is expected from very fresh water ($<700 \mu\text{S}/\text{cm}$). Previous studies suggesting that Lake Hula underwent periods of hydrological closure on the basis of relatively high covariance, however, do not explore alternative scenarios or other factors which may have contributed to oxygen-carbon covariation in the lake water (Stiller and Hutchinson, 1980; Talbot, 1990).

In studies of lacustrine carbonate records, covariant trends of carbon and oxygen isotopes have been used since the 1990s to identify the hydrological connectivity of basins and changes in basin hydrology. High degrees of $\delta^{18}\text{O}$ - $\delta^{13}\text{C}$ covariance ($r > 0.8$) are most often associated with hydrological closure and long residence times because, as residence times increase, so do opportunities for the lake water to be modified by

in-lake processes such as evaporation and in-lake productivity (Kelts and Talbot, 1990; Talbot, 1990). However, in expansive, shallow lakes the effects of evaporation can be significant even when the lake is hydrologically open. The effects of evaporation are seen clearly at JRD in the sclerochronological records of Rice et al. (2023) as the progressive enrichment of gastropod shell carbonate throughout the dry summer season. Furthermore, any changes in regional climate or ecology that result in simultaneous changes in both $\delta^{18}\text{O}$ and $\delta^{13}\text{C}$ values can potentially result in high covariance, as shown by Drummond et al. (1995).

In the JRD ostracod stable isotope record, little-to-no correlation ($|r| < 0.4$; Fig. 5) exists between the carbon and oxygen isotope measurements throughout most of the sedimentary sequence, consistent with previous interpretations of the lake as hydrologically open during the late Pleistocene. We recognize, however, that residence time is unlikely to have been constant over the study period and multiple brief intervals of high correlation are identified in the r_{500} record. When high

$\delta^{18}\text{O}$ - $\delta^{13}\text{C}$ covariance is the result of simultaneously rising $\delta^{13}\text{C}$ and $\delta^{18}\text{O}$ values we believe this to be an indication of increasing residence times under warm and arid conditions; when high $\delta^{18}\text{O}$ - $\delta^{13}\text{C}$ covariance results from the simultaneous delivery of low- $\delta^{18}\text{O}$ rainwater and low- $\delta^{13}\text{C}$ dissolved inorganic carbon (DIC) to the lake, we argue this may be indicative of high-precipitation conditions and high catchment productivity (Talbot, 1990; Drummond et al., 1995; Rice et al., 2023).

5.3. Oxygen isotope record

The long-term average values of the JRD ostracod $\delta^{18}\text{O}$ record exhibits variation within an approximately 3‰ range (Fig. 4). This narrow range of down-section variation, along with low $\delta^{18}\text{O}$ values, is consistent with models of mid-sized hydrologically-open lakes described in Talbot (1990), Leng and Marshall (2004), and Roberts et al. (2008). Greater variation in the oxygen isotopic profiles in the smaller, post-LGM lake relative to that of the larger, LGM lake reflects the heightened sensitivity to change of the smaller-volume lake (Stuiver, 1970; Leng and Marshall, 2004). The oxygen isotopic composition of lacustrine biogenic carbonates is a function of the composition of the lake water, carbonate calcification temperature, and species-specific vital effects (Craig and Gordon, 1965).

5.3.1. Lake water isotopic composition

In open lakes with relatively rapid through-flow, lake water $\delta^{18}\text{O}$ values are expected to most closely reflect the compositions of precipitation (Craig and Gordon, 1965; Leng and Marshall, 2004). Surface runoff to Lake Hula includes both springs and rivers with similar $\delta^{18}\text{O}$ values (−7.8 to −5.9‰) mainly reflecting the annual mean $\delta^{18}\text{O}$ values of precipitation in this region (Fig. 2; Gat and Dansgaard, 1972; Babad et al., 2019).

The isotopic composition of the inflows is expected to reflect the composition of the precipitation modified by fractionation processes which occur along the vapor transport pathway and during condensation (Dansgaard, 1964; Stuiver, 1970; Rozanski et al., 1993; Leng and Marshall, 2004). At JRD, low $\delta^{18}\text{O}$ values during the coldest and雨iest winter months are amplified by the lower winter temperatures as well as the increase in distillation associated with the increase in rain volume (Dansgaard, 1964). High $\delta^{18}\text{O}$ values can be associated with warmer and drier periods as evaporation is also expected to occur both over the surface of the shallow lake as well as from the surfaces of the inflowing streams. Intra-annual variability in the JRD gastropod $\delta^{18}\text{O}$ record suggests lake water enrichment on the order of 2–3‰ over the course of the summer season, with less summer evaporative enrichment occurring during the LGM than in the post-LGM period (Rice et al., 2023). During periods of low lake level it is expected that the influence of the inflows is greatest due to the shore-proximal location of JRD, resulting in the

near-constant addition of compositionally immature water (Fontes et al., 1970).

5.3.2. Lake water temperature

Lacustrine carbonate $\delta^{18}\text{O}$ values are also dependent on carbonate precipitation temperature, where calcite $\delta^{18}\text{O}$ decreases by c. 0.22‰ for every 1 °C increase in water temperature at the site of carbonate formation (Craig and Gordon, 1965). Air temperature changes at JRD, reconstructed using a pollen-based paleoclimate model by Langgut et al. (2021) show that average annual air temperatures were generally 15–17 °C during the LGM and 17–19 °C in the post-LGM period. It is therefore not possible to ascribe much of the variation seen in the long-term averaged JRD ostracod $\delta^{18}\text{O}$ record to shifts in the regional air temperature. Large differences between the same-age duplicate measurements (up to 3.5‰ for $\delta^{18}\text{O}$; Fig. 4), indicate that the lake water composition and/or temperature was less uniform on shorter time scales. In particular in the shallow-water and near-shore environments, effects of seasonal water temperature change are expected to be high (Labuhn et al., 2022). This is consistent with observations of Lake Hula in the 20th century, where monthly-averaged surface water temperatures varied on the order of c. 10 °C over the course of the year and c. 2 °C temperature differences were observed between summer bottom (2-m water depth) vs surface water (Fig. 2; Jones, 1940; Neumann, 1953).

5.3.3. Vital effects, autecology and seasonality

During the formation of the ostracod valve calcite, nonequilibrium fractionation effects attributed to biologic (metabolic) factors result in offsets between the isotopic composition of the habitat water and the valve carbonate. These effects are commonly consistent among species or even genera over time, are temperature-independent and result in species-specific offsets of up to several per mil (Xia et al., 1997; von Grafenstein et al., 1999). Although taxa-specific vital offsets have not been studied for *Ilyocyparis* specifically, we are able to compare the ostracod calcite $\delta^{18}\text{O}$ values measured here with stable isotope analyses performed on *Melanopsis* aragonite recovered from the same sediments and from which lake water isotopic compositions have been modelled (Fig. 6; Rice et al., 2023). *Melanopsis* shells are known to exhibit considerable vital effects, i.e., species-specific deviations from the $\delta^{18}\text{O}$ of inorganic carbonate which would have been precipitated in isotopic equilibrium with the lake water. Zaarur et al. (2016) report $\delta^{18}\text{O}$ values from modern *Melanopsis* shells that are, on average, 2.3‰ lower than the water in which they lived ($n = 9$). At JRD, Rice et al. (2023) also present measured mean *Melanopsis* $\delta^{18}\text{O}$ values that are lower than modelled lake water $\delta^{18}\text{O}$ values (Fig. 6). At JRD, however, the ostracod valve $\delta^{18}\text{O}$ measurements reported here are c. 2–4‰ higher than average *Melanopsis* $\delta^{18}\text{O}$ values from the same beds and c. 1–3‰ higher

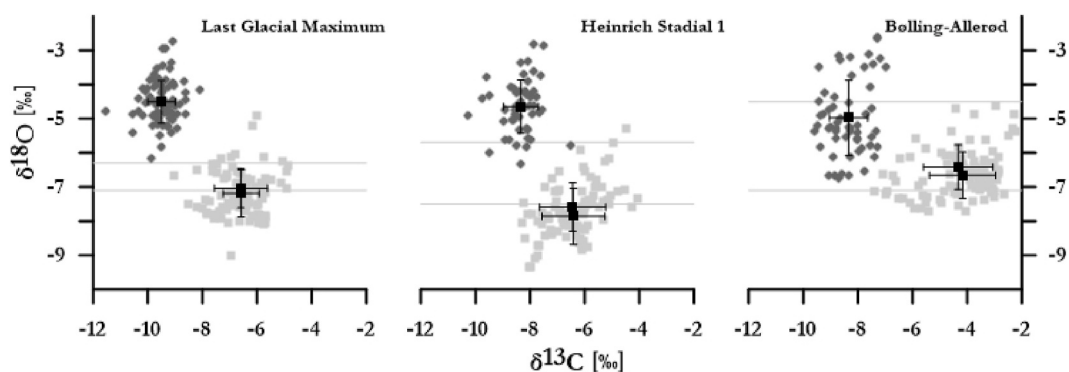


Fig. 6. Stable isotope measurements of JRD ostracods (dark grey diamonds; this study) and *Melanopsis* gastropods (light grey squares; Rice et al., 2023) during the LGM (left), Heinrich Stadial 1 (center), and Bølling-Allerød interstadial (right). The whole-shell averages for each *Melanopsis* shell and the average ostracod isotopic compositions for each period are plotted as black squares with standard deviations shown. Horizontal grey bars indicate the ranges of the modelled lake water $\delta^{18}\text{O}$ values presented in Rice et al. (2023).

than reconstructed mean Paleolake Hula $\delta^{18}\text{O}$ lake water values (Fig. 6; Rice et al., 2023). This suggests that vital effects for *Ilyocypris* may be on the order of c. +2 ‰. Differences between ostracod- and gastropod-derived stable isotope measurements likely reflect the combined effect of differences in the organisms' habitats (microenvironments) and life cycles (seasonality of the growth cycle) in addition to metabolisms/taxa-specific vital effects.

Reconstructions of rainfall seasonality at JRD show that the modern pattern of rainfall distribution—in which approximately 65 % of annual rain falls in winter—was also present throughout much of the late Pleistocene (<https://ims.gov.il/en/data.gov>; Langgut et al., 2021). At JRD, we therefore assume that most of the lake water comprises winter rain, for which the isotopic composition reflects winter conditions progressively modified by the effects of evaporation throughout the summer. In the sclerochronological modeling of Rice et al. (2023), the calcification of *Melanopsis* shells did not occur at temperatures below 14.5 °C. In the modern (20th century) Lake Hula, average monthly surface water temperatures this low only occurred in January and February (Fig. 2; Ashbel, 1945). However, under the cooler environmental conditions of the late Pleistocene (Langgut et al., 2021), the growth season for *Melanopsis* in the Hula Valley was likely shorter. For this reason, we expect the whole-shell average *Melanopsis* $\delta^{18}\text{O}$ values to overrepresent lake conditions during the warmest parts of the year. On the other hand, *Ilyocypris* at JRD may prefer cooler water conditions. In a preliminary description of ostracods from JRD, Valdimarsson (2017) identifies *Ilyocypris* cf. *bradyi* as the most abundant taxon in the sediments and reports that it is present in all samples. *Ilyocypris bradyi* is generally regarded to be both oligothermophilic and eurychronic, however, some evidence exists to suggest *I. bradyi* may not be found year-round in environments where temperatures become very warm. Olubanjo and Idowu (2024) report the absence of *Ilyocypris bradyi* from Jabi Lake (Nigeria) during the warmest months of the year. Additionally, Hussein et al. (2004) report a very strong winter preference for *I. biplicata* in freshwater canals near Luxor (Egypt), another species typically not regarded as a winter form (Meisch, 2000). In Paleolake Hula, *Ilyocypris* may have been most common during the cooler months of the year, especially during climatically warmer periods. Differences in the *Ilyocypris* and *Melanopsis* $\delta^{18}\text{O}$ values may therefore provide additional information about late Pleistocene seasonality in the Hula Valley.

At JRD, each stable isotope measurement is the average of multiple valves, and multiple measurements were performed for many of the stratigraphic levels. As *Ilyocypris* valves are known to calcify rapidly but not during any specific part of the year, we interpret our time-averaged results as being representative of average annual conditions at the centennial scale while the individual measurements provide information on the degree of variability present in the water column on shorter timescales. However, we note that the JRD ostracod stable isotope record may be slightly biased toward winter conditions during warm periods.

5.4. Carbon isotope record

The carbon isotopic compositions of benthic biogenic carbonates, such as *Ilyocypris* ostracod valves, reflect the dissolved inorganic carbon (DIC) available to them in the lacustrine environment and are further influenced by the diets, metabolisms and lifecycles of the organisms (Meisch, 2000). Furthermore, studies of other ostracod taxa typically show $\delta^{13}\text{C}$ measurements of valve carbonate to be c. 1 ‰ more positive than the surrounding DIC at temperatures 10–40 °C (Holmes and Chivas, 2002).

The decay of organic matter within the catchment and near shore environment releases DIC containing proportionally more ^{12}C decreasing the $\delta^{13}\text{C}$ values of the water. Lake water $\delta^{13}\text{C}$ is controlled by the isotopic composition of the incoming waters, modified by the progressive uptake of ^{12}C via aquatic organisms over the course of the water's residence time, resulting in the enrichment of ^{13}C as aquatic

primary productivity increases (Leng and Marshall, 2004).

Under the general climatic conditions expected at JRD during the late Pleistocene, at which time temperatures were presumably never significantly higher than they have been in recent times (Langgut et al., 2021), catchment productivity is expected to be correlated most closely with water availability. The distribution of precipitation throughout the year, specifically the length of the winter rainy season and the presence of autumn/spring precipitation, is expected to have been more important than the average annual precipitation amount. The enhanced delivery of nutrients to the basin via terrestrial runoff may also effect raising aquatic productivity, especially if these nutrients had previously only been present in limiting amounts (Van Zeist et al., 2009). Under sufficiently warm and wet conditions, the rise in $\delta^{13}\text{C}$ values expected with increased aquatic productivity is likely at least partially offset by the efficient delivery of low $\delta^{13}\text{C}$ of DIC to the lake by increased runoff, especially during times when the catchment is well-vegetated.

At JRD, variation in the ostracod carbonate $\delta^{13}\text{C}$ profile therefore reflects changes in lake (aquatic) and catchment (terrestrial) productivity as they are related to temperature and runoff. Low ostracod carbonate $\delta^{13}\text{C}$ values likely reflect periods of low aquatic productivity caused by cold water conditions or the delivery of large amounts of carbon-12 to the lake under wet conditions. High $\delta^{13}\text{C}$ values can be caused by low rates of carbon recycling in the catchment, low-precipitation conditions, and high aquatic productivity. A substantial contraction of the lake at c. 17.2 ± 0.1 cal ka BP as well as smaller-amplitude changes in the lake volume during the Bølling-Allerød and Younger Dryas are known from previous geological investigations of the JRD site (Björvinsson, 2017; Valdimarsson, 2017; Rice et al., 2023; Bunin et al., 2024). In this smaller lake, post-LGM warming led to an increase in aquatic productivity reflected in generally higher $\delta^{13}\text{C}$ values, though with more variability. These generally higher $\delta^{13}\text{C}$ values are suggested to reflect higher aquatic productivity under warmer, post-LGM conditions. We propose that local minima in the $\delta^{13}\text{C}$ record of this smaller lake resulted from the delivery of low- $\delta^{13}\text{C}$ terrestrial DIC to the lake by streams, especially during times when the catchment was well-vegetated and the influence of streams near the sampling site was high. Additionally, decreasing $\delta^{13}\text{C}$ values occur at the bases of Beds 5, 7 and 9 and were associated with increases in water level at JRD (Bunin et al., 2024).

5.5. The $\delta^{18}\text{O}$ sea-land relationship at JRD

Average temperature-corrected $\Delta \delta^{18}\text{O}_{\text{sea-land}}$ is 7.4 ± 1.1 ‰ for all samples, 8.4 ± 0.7 ‰ during the LGM (21.1 ± 0.2 to 18.0 ± 0.1 cal ka BP) and 6.9 ± 0.9 ‰ for the post-LGM period (c. 17.2 ± 0.1 to 11.3 ± 0.2 cal ka BP; Fig. 7). The period 18.0 ± 0.1 to 17.0 ± 0.1 cal ka BP is excluded due to low temporal resolution of the JRD record during this interval. Differences between the isotopic composition of the Mediterranean Sea source water and the terrestrial oxygen isotopic records of the southern Levant ($\Delta \delta^{18}\text{O}_{\text{sea-land}}$) result from fractionation processes which occur during the evaporation, transport, and precipitation of meteoric water over the inland landscapes of the southern Levant (Bar-Matthews et al., 2003; Almogi-Labin et al., 2009). In our source-corrected $\delta^{18}\text{O}$ record, most periods of high or rising $\Delta \delta^{18}\text{O}_{\text{sea-land}}$ values are correlated with periods of relatively high or rising water levels at JRD, and broadly parallel the lake level curve established for this site (Bunin et al., 2024). When water levels were very low, however, low $\delta^{18}\text{O}$ and/or large $\Delta \delta^{18}\text{O}_{\text{sea-land}}$ values may reflect the influence of local streams, especially during periods of enhanced sand and terrestrial material deposition such as in Bed 11. At JRD, high (low) $\Delta \delta^{18}\text{O}_{\text{sea-land}}$ values are thus interpreted as reflecting high- (low-)precipitation conditions in the Hula Valley watershed. During wet periods, high $\Delta \delta^{18}\text{O}_{\text{sea-land}}$ values are likely amplified by the amount effect, in which the $\delta^{18}\text{O}$ value of precipitation is more negative in rainy months relative to drier months (Dansgaard, 1964). When compared to lake level curves for Paleolake Hula and Paleolake Lisan, the JRD $\Delta \delta^{18}\text{O}_{\text{sea-land}}$ record

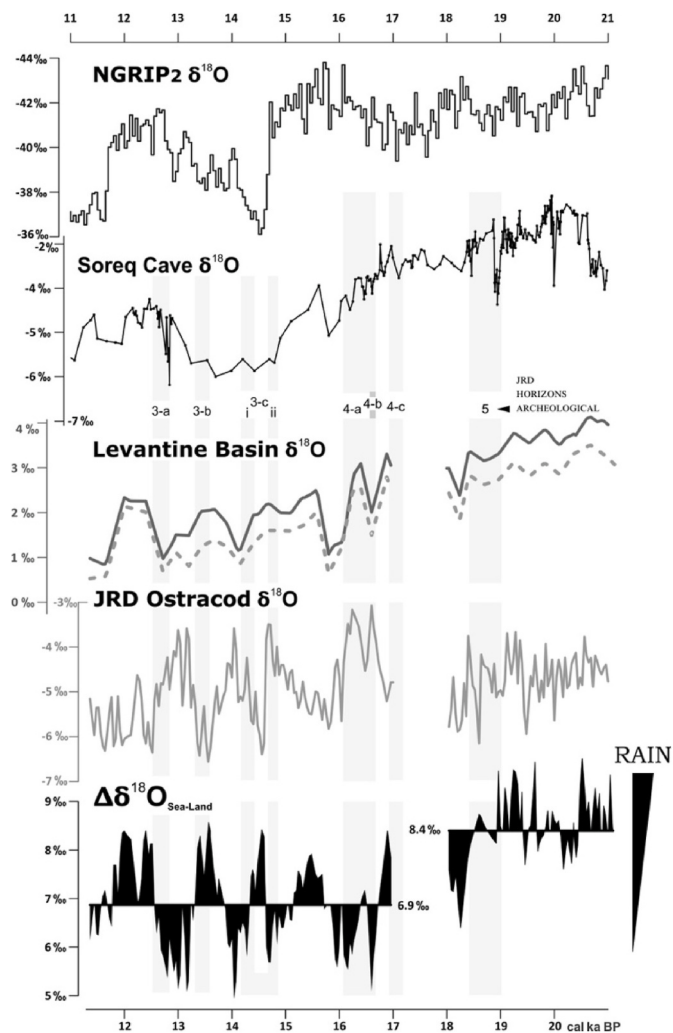


Fig. 7. Oxygen isotope compositions of (top to bottom) the North Greenland Ice Core Project core 2 (NGRIP2, note reversed y-axis; Rasmussen et al., 2014; Seierstad et al., 2014), Soreq Cave (Grant et al., 2012), Levantine Basin sediment core MD95-9501 (Almogi-Labin et al., 2009) corrected for sea surface temperature (solid line) and uncorrected (dashed line), JRD ostracods (this study) and the $\Delta\delta^{18}\text{O}_{\text{Sea-Land}}$ values for JRD relative to core 9501 (this study). Data from NGRIP2 (50 year means) are plotted using the GICC05modelext timescale (Seierstad et al., 2014). JRD archeological horizons from Sharon et al. (2020).

shows that water level change in the lakes along the Dead Sea Transform is controlled by changes in the precipitation-evaporation balance of the lake, which are themselves driven by changing precipitation amounts in the Hula Valley watershed (so-called pluviosity; Fig. 7).

5.6. Inferred late Pleistocene paleoenvironmental conditions in the Hula Valley

5.6.1. Last Glacial Maximum and early deglaciation – up to 17.2 ± 0.1 cal ka BP (JRD Beds 1–3)

The LGM of the southern Levant is generally accepted to have been a time of cooler temperatures and reduced precipitation relative to the present (Goodfriend and Magaritz, 1988; McGarry et al., 2004; Langgut et al., 2021) despite high water levels in the lakes of the Dead Sea Transform. Whether these high lake levels were the result of greatly suppressed evaporation or high precipitation has been the subject of much discussion recently (Torfstein et al., 2013; Miebach et al., 2019; Rice et al., 2023) as has the timing of the maximum high-stand and subsequent lake level drop (Jara-Muñoz et al., 2024). At JRD, high

discharge of water to the paleolake has been inferred from the sedimentary record, which includes abundant terrestrial material containing ancient foraminifera derived from the mountain ranges to the west and north, large pieces of charcoal, and abundant silt (Fig. 3). This material was presumably delivered to the lake bed by incoming streams—including the nearby Mahanayim Stream (Fig. 2)—powerful enough to rapidly transport this material to shore-distal positions, as evidenced by elevated sedimentation rates during the LGM and early deglaciation (Bunin et al., 2024). The inferred large discharge of water to Paleolake Hula is seemingly at odds with the low-precipitation conditions shown in the pollen-based environmental reconstruction of Langgut et al. (2021). In the Hula Valley, relatively high lake levels and fluvial input may have been caused by an increase in runoff unrelated to eastern Mediterranean-derived precipitation falling in the valley itself, for example, from snow/ice melting or rain falling in the upper reaches of the catchment (Ayalon et al., 2013; Zaarur et al., 2016; Rice et al., 2023).

In the Hula Valley, the LGM was likely cool and wet, and Paleolake Hula existed as an open lake with a volume significantly larger than has been observed in modern times (Fig. 2). Low aquatic productivity under cool conditions is likely responsible for lower ostracod carbonate $\delta^{13}\text{C}$ values in the LGM paleolake. No significant $\delta^{18}\text{O}$ - $\delta^{13}\text{C}$ covariation is observed in the JRD LGM sediments, consistent with the current understanding that Paleolake Hula was a mid-sized, well-buffered, hydrologically-open system throughout this time (Rice et al., 2023; Bunin et al., 2024). Minimal variation in $\delta^{18}\text{O}$ values is consistent with the expected behavior of a mid-sized exorheic lake, where the lake water $\delta^{18}\text{O}$ values are less prone to be affected by short-term fluctuations in air temperature due to increased thermal capacity of the larger lake and less likely to be influenced by sudden influxes of freshwater due to increased distance between the sampling site and the stream inflows (Fontes et al., 1970; Talbot, 1990; Kolodny et al., 2005). High $\delta^{18}\text{O}$ values with little variation during the LGM and early deglaciation reflect the composition of eastern Mediterranean Sea surface water, where surface water $\delta^{18}\text{O}$ values were between +2 and +3‰ at this time (Fig. 7). In the eastern Mediterranean, lower Mediterranean Sea levels during glacial periods (Thiede, 1978, Fig. 1) increase the distance between the coastline and JRD, and therefore the effects of Rayleigh distillation. This led to lower rainfall $\delta^{18}\text{O}$ values over the inland Levant during periods of low sea level (Bar-Matthews et al., 2003; Almogi-Labin et al., 2009). However, these are offset by higher starting $\delta^{18}\text{O}$ values of the vapor source, as shown by higher-than-average $\Delta\delta^{18}\text{O}_{\text{sea-land}}$ values calculated for glacial periods: on average, $\delta^{18}\text{O}$ values in the LGM portion of the JRD record are only slightly higher (0.3‰) than those of the post-LGM period. During the LGM, JRD $\Delta\delta^{18}\text{O}_{\text{sea-land}}$ values were 8.4 ± 0.7 ‰ for the period 21.1–18.0 cal ka BP. This is c. 1‰ higher than the general late Pleistocene average $\Delta\delta^{18}\text{O}_{\text{sea-land}}$ value at JRD (7.4 ± 1.1 ‰) and higher than LGM $\Delta\delta^{18}\text{O}_{\text{sea-land}}$ values reported for other records from the southern Levant (c. 5.5–6.5‰; Bar-Matthews et al., 2003; Almogi-Labin et al., 2009). Larger $\Delta\delta^{18}\text{O}_{\text{sea-land}}$ values at JRD relative to Soreq Cave therefore reflect higher precipitation conditions in the north relative to south and central portions of the Lake Lisan watershed and confirm the importance of northern sources of the precipitation in controlling Lake Lisan water levels during this time (Bar-Matthews et al., 2003; Almogi-Labin et al., 2009).

5.6.2. Heinrich Stadial 1: c. 17.2 ± 0.1 – 14.7 ± 0.2 cal ka BP (JRD Beds 4–7)

At 17.2 ± 0.1 cal ka BP, a sudden drawdown in Paleolake Hula water level occurred, resulting in the shift from a relatively large and hydrologically open waterbody during the LGM to a smaller and poorly-buffered lake afterwards (Rice et al., 2023; Bunin et al., 2024). At JRD, this drawdown coincided with sudden increases in both sand deposition (Bunin et al., 2024) and $\delta^{13}\text{C}$ values (a rise of approximately 1.5‰; this study). Sand deposition likely reflects the increasing influence of streams at the study site as the paleoshoreline migrated closer to

JRD. The sudden increase in $\delta^{13}\text{C}$ values at 17.2 ± 0.1 cal ka BP is suggested to indicate a rise in the primary productivity of the lake under warmer post-LGM conditions and/or a coeval reduction in runoff or groundwater inflow under dryer conditions. Increased variability in both the $\delta^{18}\text{O}$ and $\delta^{13}\text{C}$ records after 17.2 ± 0.1 cal ka BP likely reflects the decreased capacity of the smaller, late glacial lake to buffer changes in the isotopic composition of the lake water, the increasing influence of local streams, and the greater variability of the late glacial climate system.

The cause of the water-level drop itself is unknown, but evidence for a similar drawdown is reported from some studies of Lake Lisan at approximately the same time (Stein et al., 1997; Bartov et al., 2003; Torfstein et al., 2013), where it has been interpreted as evidence for a drop in precipitation following the LGM. Newly dated shoreline deposits suggest that water levels at Lake Lisan had already fallen significantly several thousand years prior (Jara-Muñoz et al., 2024). The drop in the level of Paleolake Hula may reflect a decrease in the amount of the water flowing to the lake, as a reduction in precipitation and/or meltwater coming from the north, or it may reflect an increase in evaporation, which was previously suggested by Ludwig and Hochman (2022) to have controlled lake water levels in the Levant at this time. At JRD, some $\delta^{18}\text{O}$ - $\delta^{13}\text{C}$ covariation is seen in Beds 5 and 6 (Fig. 6), suggesting that increasing evaporation did play some role in the falling post-LGM lake levels. However, this signal lags behind the shift from deep-to-shallow water sedimentary facies by hundreds of years, suggesting that the water level drop was instigated by a shift to lower discharge, either in the form of reduced precipitation or meltwater reaching the lake. In Beds 4 and 6 (c. 17.2 ± 0.1 to 16.0 ± 0.2 cal ka BP), local maxima in the $\delta^{18}\text{O}$ record along with low $\Delta \delta^{18}\text{O}_{\text{sea-land}}$ values in Bed 6, are attributed to a low contribution of meteoric water and low precipitation-evaporation balance during times of lake level low stands. Together with the elevated $\delta^{13}\text{C}$ values, suggested here to reflect a combination of low organic carbon recycling in the catchment and reduced runoff, a return to cold and dry conditions is inferred for the first half of the stadial. This is consistent with the characterization of this time period presented in Langgut et al. (2021), who describe low temperatures and a decline in winter precipitation for this time, as well as relatively low water levels reconstructed for Paleolake Hula in Bunin et al. (2024).

At 16.1 ± 0.2 cal ka BP, the sudden drops in both $\delta^{18}\text{O}$ and $\delta^{13}\text{C}$ values (a spike in $\Delta \delta^{18}\text{O}_{\text{sea-land}}$ values) at the base of Bed 7 are interpreted as an increase in precipitation, consistent with the rise in water level previously reconstructed at the base of Bed 7 in Bunin et al. (2024). This increase in precipitation is not apparent in the pollen record of the lake (Langgut et al., 2021), perhaps because it was short-lived. Toward the end of Heinrich Stadial 1, rising $\delta^{18}\text{O}$ values (shrinking $\Delta \delta^{18}\text{O}_{\text{sea-land}}$ values) from 15.8 ± 0.2 to 14.7 ± 0.2 cal ka BP are attributed to a combination of decreasing precipitation and increasing evaporation, which likely resulted in a progressive reduction in the lake size. By 15.3 ± 0.2 cal ka BP, the dominant lithology of the sediments had changed from silt to sandy silt as the paleoshoreline receded and the position of JRD became more shore-proximal, and by 14.9 ± 0.2 cal ka BP, the water level at JRD had dropped enough to support a dense community of shallow-water bivalves (Bunin et al., 2024).

5.6.3. Bølling-Allerød Interstadial: 14.7–12.9 cal ka BP (JRD Beds 8–11)

At 14.7 cal ka BP, the start of the Bølling-Allerød interstadial coincides with a sudden drop in excess of 2‰ in the $\delta^{18}\text{O}$ values at JRD as well as a decrease in $\delta^{13}\text{C}$ values and a spike in the $\Delta \delta^{18}\text{O}_{\text{sea-land}}$ record. This is suggested to reflect a sudden increase in precipitation at the site at the start of the interstadial, although other regional records have interpreted a similarly timed large drop in $\delta^{18}\text{O}$ values as evidence for an abrupt change in the isotopic composition of the precipitation (Rowe et al., 2012). Because of the rapid onset of the interstadial, no $\delta^{18}\text{O}$ - $\delta^{13}\text{C}$ covariation is seen in our record as it is expected to not be visible at this

scale. Warm and wet conditions during the Bølling-Allerød interstadial are also reconstructed from the Hula Valley pollen record of Langgut et al. (2021), who model a temperature increase of approximately 3°C for this time. At JRD, falling $\delta^{18}\text{O}$ values and high $\Delta \delta^{18}\text{O}_{\text{sea-land}}$ values likely integrate the signal of increasing stream influence in a shore proximal environment and an increase in freshwater input to the lake as precipitation as was suggested in Langgut et al. (2021). This initial increase in freshwater input is visible in the lithostratigraphic record of JRD as a lens of sediments containing less sand and shells contained within Bed 8 (between archeological horizons 3ci and 3cii), suggestive of deposition in a deeper-water environment (Fig. 4; Sharon et al., 2020). The increasing influence of freshwater streams at JRD is also inferred from the lake water conductivity transfer function results of Valdimarsson (2017), who reconstructed a c. 10% reduction in conductivity (salinity) at 14.6 ± 0.2 cal ka BP, as well as with the palynological record of Van Zeist et al. (2009), who notes high discharge to the lake at this time.

At JRD, there is less contrast between the gastropod (spring-summer-fall carbonate accretion) and ostracod $\delta^{18}\text{O}$ values (year-round calcification) during the Bølling-Allerød relative to the LGM and Heinrich Stadial 1 (Figure 6). This may indicate warmer winter conditions and less seasonality contrast during the Bølling-Allerød (relative to the LGM and Heinrich Stadial 1), which has also been inferred from the pollen record presented in Langgut et al. (2021). This is consistent with the observations of Denton et al. (2005), where seasonality is greatest in cold episodes.

5.6.4. Younger Dryas Stadial: 12.9 ± 0.1 – 11.7 ± 0.2 cal ka BP (JRD Beds 12 and 13)

The onset of the Younger Dryas coincides with the lower boundary of JRD Bed 12. Here, low precipitation and/or high evaporation is inferred from the lithology of Bed 12 along with the low $\Delta \delta^{18}\text{O}_{\text{sea-land}}$ values. A dry and cold early Younger Dryas is also known from the pollen study of Langgut et al. (2021). An increase in the eastern Mediterranean Sea $\delta^{18}\text{O}$ values corresponds to the boundary between Bed 12 and Bed 13 and an increase in precipitation at JRD which is visible in the $\Delta \delta^{18}\text{O}_{\text{sea-land}}$ record. The shift to wetter conditions accelerated after 12.6 ± 0.1 cal ka BP, resulting in higher lake levels during the deposition of Bed 13 in addition to lower $\delta^{18}\text{O}$ values. A decrease in conductivity (salinity) between Beds 12 and 13 is also reconstructed in Valdimarsson (2017), consistent with an increase in freshwater input to the lake sometime after 12.7 ± 0.1 cal ka BP.

Sediments in Beds 12 and 13 contain abundant coarse clasts, including cobble-sized limestone and basalt clasts, foraminifera, and charcoal, indicating significant fluvial influence and shoreline proximity, which we interpreted in a previous study as an indication of low water levels during the Younger Dryas (Bunin et al., 2024) and attributed to an increase in windiness and therefore evaporation, as suggested in Roskin et al. (2011). However, we do not see any signal of evaporative enrichment in the $\delta^{18}\text{O}$ record here and therefore suggest that this drop in lake level does in fact reflect a decrease in watershed rainfall, which is also reflected in the low $\Delta \delta^{18}\text{O}_{\text{sea-land}}$ values during the deposition of Bed 12. The shoreline transgression reconstructed for Bed 13 corresponds to high $\Delta \delta^{18}\text{O}_{\text{sea-land}}$ values which appear to reflect a shift to wetter conditions in the later half of the Younger Dryas. Here, the large number of clasts and terrestrial matter deposited, along with the low $\delta^{18}\text{O}$ values of the ostracod valves may indicate that a stream outlet was present close to the sampling site, though the site appears to be in a fairly shore-distal position here. Following the Younger Dryas, a drop in the eastern Mediterranean Sea water $\delta^{18}\text{O}$ values partly masks a rise in ostracod $\delta^{18}\text{O}$ values at the beginning of the Holocene, which may have been very dry here (Fig. 7).

5.7. Connection with North Atlantic climate

Variation within the JRD ostracod $\delta^{18}\text{O}$ record appears to exhibit

some correlation with centennial- and/or millennial-scale variability observed at other sites in the circum-Mediterranean region and elsewhere in the Northern Hemisphere (Fig. 7). Cycles of rising and falling $\delta^{18}\text{O}$ values over the course of the Late Pleistocene appear similar to the oxygen isotope records published for the Greenland ice cores, where negative excursions in the Greenlandic $\delta^{18}\text{O}$ records are associated with cold periods (Fig. 7; Rasmussen et al., 2014). These cold periods correspond to times of high $\delta^{18}\text{O}$ values in the post-LGM JRD record, interpreted as periods of low precipitation. This is consistent with other records of millennial-scale (hydro)climate variability from the western and central Mediterranean where precipitation amounts are controlled by Atlantic Meridional Overturning Circulation strength and ultimately by North Atlantic temperatures (Stockhecke et al., 2016; Grant et al., 2016; Columbu et al., 2022; Incarbona et al., 2022). In the eastern Mediterranean, correspondence between the Greenland ice core records and inverse Levantine Basin sediment core (foraminiferal) $\delta^{18}\text{O}$ values has also previously been reported by Almogi-Labin et al. (2009). They observed that low *Globigerinoides ruber* $\delta^{18}\text{O}$ values occurred together with high NGRIP $\delta^{18}\text{O}$ values at the inception of the Bølling-Allerød but that high *G. ruber* $\delta^{18}\text{O}$ values were associated with the large negative $\delta^{18}\text{O}$ excursion reported at c. 13.2 ka in the NGRIP record, the peak of the Glacial Interstadial 1b cool phase (Rasmussen et al., 2014). At JRD, generally drier conditions are reconstructed for many of the globally cool phases of the late glacial, including early Heinrich Stadial 1 (c. 16.6–16.0 cal ka BP), Glacial Interstadial cool phases 1b and 1d and the early Younger Dryas Stadial (Fig. 7). This is suggested to reflect the reduced strength of the westerlies during these times, which manifests as a decrease in winter precipitation. Although summer storms are inferred to have been more frequent during early Heinrich Stadial 1 (Langgut et al., 2021; Rice et al., 2023), they are unlikely to have significantly affected the ostracod stable isotope record as it is most likely dominated by the winter precipitation signal since winter precipitation is expected to have comprised most of the lake volume throughout the late glacial (Langgut et al., 2021).

5.8. Paleoenvironmental context of Epipaleolithic cultural evolution

The Hula Valley is home to some of the Levant's most important Epipaleolithic sites. Human presence there is well-documented throughout the LGM and late glacial. Here, key large sites such as Eynan (Natufian; Valla et al., 2017) and Beisamoun (PPNB; Bocquentin et al., 2014, PPNB), as well as several smaller sites (Sharon et al., 2018), collectively document one of the most significant cultural shifts of human history: the transition from small, mobile groups of hunter-gatherers during the LGM to the large, settled agricultural communities of the Neolithic. The seemingly continuous presence of humans on this landscape suggests that, although the late glacial was a period of dramatic climatic changes globally, local conditions were always suitable (and sometimes even optimal) for human habitation. Resources, in the form of water or food, do not appear to have ever been scarce in the Hula Valley.

In archeological contexts, paleoenvironmental studies are often designed to detect parallel changes in environmental proxies and use them to explain the cultural record. However, changes in climate and culture are not necessarily simultaneous or related, and care should be taken when interpreting shifts in environmental conditions as driving cultural change (Arponen et al., 2019). This is especially important when environmental changes as shown to be subtle, as they are here. With this in mind, we examine local environmental conditions in the Hula Valley during two important changes visible in the JRD archeological record: the transition from the Early Epipaleolithic Mazraqan culture to the Middle Epipaleolithic Geometric Kebaran culture and the transition from the Geometric Kebaran to the Late Epipaleolithic Natufian. Culturally, this is a dramatic shift, as the Natufian culture established the first settlements and are the precursors of the Neolithic agricultural way of life (Bar-Yosef and Belfer-Cohen, 1989; Belfer-Cohen

and Bar-Yosef, 2000). We note that, at JRD, cultural horizons are separated by beds of archeologically sterile sediments deposited during periods of higher lake level. Such clear separation of lithic tradition horizons is rarely seen in archeological sites. Because of this stratigraphic arrangement, we are not able to observe whether transitions between the phases of the Epipaleolithic occurred gradually or suddenly, or pinpoint timings of the transitions beyond noting the first and last appearances of the various lithic traditions.

At JRD, the transition from the Early to Middle Epipaleolithic occurred sometime between 18.4 ± 0.1 and 17.2 ± 0.1 cal ka BP (Bed 3, Figs. 3 and 4). In the Lake Hula record, this period was characterized by a shift to warmer temperatures, drier conditions and specifically a reduction in summer precipitation, as shown in the pollen record and vegetation modeling of Langgut et al. (2021). Globally this period corresponds to the late glacial (post-LGM) warming which immediately preceded Heinrich Stadial 1 (GS2.1a; Rasmussen et al., 2014). In the Hula Valley, this warming and drying trend ultimately raised annual average temperatures by approximately 4°C , contributing to the increased evaporation over the waterbodies of the Dead Sea Transform that ultimately culminated in the lake level drawdown/volume reduction that occurred at c. 17.2 ± 0.1 cal ka BP (Langgut et al., 2021; Bunin et al., 2024). The Early-to-Middle Epipaleolithic transition is also associated with aridification and the size reduction of a local freshwater body at Kharaneh IV, in central Jordan, although the Early-to-Middle Epipaleolithic transition occurred earlier at that site (Macdonald et al., 2018).

The transition from the Middle to Late Epipaleolithic at JRD occurred sometime between 16.0 ± 0.1 and 14.8 ± 0.1 cal ka BP (Bed 7, Figs. 3 and 4). Although this period is characterized by an initial, sudden increase in freshwater input and lake level at 16.0 ± 0.1 cal ka BP, seen as a sudden drop in ostracod carbonate $\delta^{18}\text{O}$ values and a shift to more shore-distal sediment deposition, it is immediately followed by a 900-year drying trend starting at c. 15.8 ± 0.2 cal ka BP, inferred from steadily increasing ostracod carbonate $\delta^{18}\text{O}$ values (this study) and also visible in the palynological record and modelling of Langgut et al. (2021) as a decline in annual precipitation and the expansion of dwarf-shrub steppe vegetation (Pollen Zone 3). This drying resulted in the gradual contraction of the lake, as inferred from changes in the sediment lithology and microfossil content (Bunin et al., 2024; this study). By 14.8 cal ka BP, the water column at JRD was shallow enough that humans had recommenced fishing activities here, this time using tools typical of the Natufian culture (Bunin et al., 2024; Pedergana et al., 2021; Sharon et al., 2020). While we can only infer that the shift from Middle to Late Epipaleolithic occurred sometime between 16.0 ± 0.1 and 14.8 ± 0.2 cal ka BP at JRD, we note that the most recent chronologies of Natufian place this transition toward the end of Heinrich Stadial 1 (the Older Dryas), at 15.0 ± 0.2 cal ka BP, corresponding to a time that we show here to have experienced less and less rain in the Hula Valley for hundreds of years (Grootes and Stuiver, 1997; Belfer-Cohen and Goring-Morris, 2020). While it is interesting to note that the transition from both the Early to Middle and Middle to Late Epipaleolithic periods took place against the backdrop of locally-dryer conditions in the Hula Valley, at this stage, very little can be said about the role environmental change may have played, if any at all, in bringing about any form of cultural change. Despite identifying two periods of declining precipitation that may correspond to turnovers in the cultural entities occupying JRD, the magnitudes of these changes in the Hula Valley were modest and resulting environmental shifts were unlikely to have been sudden or severe enough to cause significant stress for communities living in the valley. Thus, our results do not support the hypothesis that the dramatic cultural changes of the Epipaleolithic in the Mediterranean zone of the Levant occurred in direct response to worsening environmental conditions or volatility experienced by prehistoric hunter-fisher-gatherers (Bar-Yosef and Belfer-Cohen, 1989; Wright, 1993; Ashraf and Michalopoulos, 2015).

At JRD, fishing equipment is found throughout the record and the

focus on small-game and aquatic resources is consistent with models of subsistence intensification published for the Mediterranean Zone of the Levant (Sharon et al., 2020; Pedergnana et al., 2021). These models often propose that human diet diversification occurs in response to resource depression resulting from either worsening environmental conditions or increasing human populations (Binford, 1968; Flannery, 1969). Because evidence for fishing is present even in the earliest horizons of the JRD record, it is not possible to determine which environmental conditions were present at the time fishing was first practiced in the Hula Valley. It is clear, however, that once fishing began, it was practiced regularly here for thousands—or even hundreds of thousands—of years (Zohar and Biton, 2011). While much work remains to be done in characterizing the breakdown of the late Pleistocene human diet and its evolution over the course of the Epipaleolithic, it appears that environmental changes reconstructed for the Hula Valley were not severe enough to have forced any significant dietary changes (Langgut et al., 2021; this study).

While our study shows that the Hula Valley experienced fluctuations in temperature, precipitation and seasonality which are clearly visible in the JRD proxy records, local conditions in the Hula Valley remained favorable for human habitation and resources appear to have been abundant throughout the Epipaleolithic. Despite relative environmental stability reconstructed here for the Hula Valley, in other parts of the southern Levant, however, climate may have been considerably more volatile, and periods of adverse conditions may have driven humans and other animals to seek out more favorable habitats elsewhere, as was recently suggested in Stein et al. (2025) for Heinrich Stadial 1. It is possible that the mesic Hula Valley, with its mild summers, relatively abundant precipitation and significant resources, served as one such destination during periods of adverse environmental conditions elsewhere.

Despite being clearly visible in our proxy records, the gradual, low-magnitude hydroclimate changes reconstructed here likely were subtle enough and occurred slowly enough that they were not a significant source of stress for the Hula Valley's Epipaleolithic inhabitants. It is even possible that these subtle changes in temperature and precipitation passed by largely unnoticed, especially as it does not appear that they impacted the availability of food or water here. It seems that for its inhabitants, the Hula Valley was a suitable habitat flush with resources consistently throughout the Epipaleolithic. For this reason, our record does not indicate that the cultural changes seen here were a response to environmental stress and alternative explanations for these shifts in human lifeways should continue to be sought (Shavit and Sharon, 2023).

6. Summary and conclusions

The oxygen stable isotope record at JRD reflects the complex interplay of numerous controls, but primarily reflects local changes in precipitation amounts and the overall precipitation-evaporation balance of the Hula Valley superimposed on the geochemical signature of the precipitation vapor source. Although the oxygen isotopic composition of the lake water exhibits considerable similarity with the record of the eastern Mediterranean Sea surface—supporting previous studies that identified the eastern Mediterranean as the vapor source of much of Northern Israel's precipitation during the late Pleistocene—changes in the lake's size ultimately control the response of the carbonate isotopic records to environmental changes.

During the Last Glacial Maximum, when paleolake Hula existed as a larger, hydrologically open lake, smaller fluctuations in the ostracod carbonate $\delta^{18}\text{O}$ record reflect the increased ability of the lake to buffer changes in temperature and water chemistry. During the post-LGM period, when the lake was smaller, its reduced volume resulted in less thermal and chemical buffering capacity, seen as larger variations in the ostracod valve carbonate $\delta^{18}\text{O}$ and $\delta^{13}\text{C}$ values, which reflect changes in the local hydrological cycle. The decreased distance between the study site and lake shoreline during periods of shoreline regression also

amplified the signals of freshwater input in the nearshore environment. When low or falling $\delta^{18}\text{O}$ values and rising lake levels occurred together with an increase in the delivery of silt-sized terrestrial material to the study site and/or low $\delta^{13}\text{C}$ values, we interpret this as evidence for increased freshwater input to the lake, as precipitation (though not necessarily in the immediate vicinity of the lake) and meltwater. When low $\delta^{18}\text{O}$ values occur during times of shoreline proximity, together with poorly sorted sediments containing cobble-sized basalt clasts, these low $\delta^{18}\text{O}$ values are attributed to the proximity of the sampling site to the inlets of spring-fed streams continuously discharging low- $\delta^{18}\text{O}$ water to the lake. Under warm and/or dry conditions, signals of evaporative enrichment in the lake water may be masked by a decrease in $\delta^{18}\text{O}$ values due to higher lake water temperatures or by the continuous delivery of low- $\delta^{18}\text{O}$ spring water to the sampling site under shore-proximal conditions.

The carbon isotopic record reflects primarily the productivity occurring within the lake, with lower $\delta^{13}\text{C}$ values during the LGM reflecting low productivity under cooler conditions and a sudden rise in the $\delta^{13}\text{C}$ values after 17.2 ± 0.1 cal ka BP reflecting an increase in productivity during warmer, post-LGM conditions. Second-order changes in the ostracod $\delta^{13}\text{C}$ values of the smaller, post-LGM lake primarily record changes in the local hydrological cycle, with the lake water $\delta^{13}\text{C}$ values reflecting the amount of water entering the lake (pluviosity) and carbon isotopic composition of the incoming streams reflecting terrestrial productivity of the catchment.

One of the most challenging aspects of interpreting stable isotope records from open lacustrine systems remains the large number of independent factors which contribute to the final isotopic composition of the carbonate, and which frequently cannot be deconvolved effectively (Develle et al., 2010). For this reason, it is necessary to consider carbonate stable isotope records in conjunction with other proxies that provide independent evidence for changes in temperature, precipitation and evaporation. The results of this study highlight the complexity and sensitivity of hydrologically-open small and medium sized lake systems and also demonstrate the need for carbonate stable isotope records to be interpreted together with other proxies such as grain-size distribution, geochemical and micropaleontological data. As this record of more than 10,000 years of lacustrine sediment deposition under a variety of conditions exhibits only modest changes in its isotopic composition, micropaleontology and sediment characteristics, we infer that environmental conditions in the Hula Valley were likely stable and attractive to humans throughout the time period investigated and that Paleolake Hula maintained a continuous presence on the Epipaleolithic landscape of the southern Levant where it was an important water source for human and animal populations of this valley during times of dramatic cultural changes in human history.

Author contribution

Elizabeth Bunin; Writing – original draft; Writing – review & editing; Funding acquisition; Investigation; Formal Analysis. Gonen Sharon; Conceptualization; Resources; Funding acquisition; Writing – review & editing. Birgit Schröder; Methodology; Investigation; Resources; Writing – review & editing. Steffen Mischke; Conceptualization; Funding acquisition; Supervision; Writing – review & editing.

Declaration of competing interest

The authors declare that they have no known competing financial interests or personal relationships that could have appeared to influence the work reported in this paper.

Acknowledgements

E. Bunin gratefully acknowledges support provided by the Icelandic Centre for Research (Ranníð) by way of an Icelandic Research Fund

Doctoral Student Grant (195689-051) and from the Israeli Council for Higher Education via the Planning and Budgeting Committee PhD fellowship program. The JRD excavation has been supported by the following grants: The Israel Science Foundation (Grant #918/17), The Brennan Foundation (two grants), The Wenner-Gren Foundation, National Geographic Society, Irene Levi Sala Care Archaeological Foundation, Tel-Hai College and MIGAL research institute research grants (all Sharon), and the University of Iceland Research Fund (Mischke). We also wish to thank Miryam Bar-Matthews and Ahuva Almogi-Labin for sharing data from core 9501. This manuscript has benefitted greatly from the detailed and constructive comments of Andrea Columbu, handling editor Donatella Magri and one anonymous reviewer, who we also wish to thank. Finally, we are grateful to the members and workers of Kibbutz Gadot for their hospitality and support during fieldwork at JRD.

Appendix A. Supplementary data

Supplementary data to this article can be found online at <https://doi.org/10.1016/j.quascirev.2025.109621>.

Data availability

All data and/or code is contained within the submission.

References

- Abadi, I., Grosman, L., 2019. Sickle blade technology in the late natufian of the Southern Levant. In: Webb, J.M., Frankel, D. (Eds.), Near Eastern Lithic Technologies on the Move: Interactions and Contexts in Neolithic Traditions. Astrom Editions, Nicosia, pp. 295–304.
- Almogi-Labin, A., Bar-Matthews, M., Shriki, D., Kolovsky, E., Paterne, M., Schilman, B., Ayalon, A., Aizenshtat, Z., Matthews, A., 2009. Climatic variability during the last ~90 ka of the southern and northern Levantine Basin as evident from marine records and speleothems. *Quat. Sci. Rev.* 28, 2882–2896.
- Alpert, P., Shay-El, Y., 1994. The moisture source for the winter cyclones in the Eastern Mediterranean. *Isr. Meteorol. Res. Pap.* 5, 20–27.
- Arponen, V.P.J., Dörfler, W., Feeser, I., Grimm, S., Grob, D., Hinz, M., Knitter, D., Müller-Scheefel, N., Ott, K., Ribiero, A., 2019. Environmental determinism and archaeology. Understanding and evaluating determinism in research design. *Archaeol. Dialogues* 26, 1–9.
- Ashbel, D., 1945. Temperature conditions of the sweet-water lakes of Palestine (in Hebrew). *Ha Teva* 2, 72.
- Ashbel, D., 1951. Regional climatology of Israel. Department of Meteorology. The Hebrew University of Jerusalem, p. 244 in Hebrew.
- Ashraf, Q., Michalopoulos, S., 2015. Climatic fluctuations and the diffusion of agriculture. *Rev. Econ. Stat.* 97 (3), 589–609.
- Ayalon, A., Bar-Matthews, M., Frumkin, A., Matthews, A., 2013. Last glacial warm events on Mount Hermon: the southern extension of the Alpine karst range of the east Mediterranean. *Quat. Sci. Rev.* 59, 43–56.
- Bar-Matthews, A., Burg, A., Adar, E.M., 2019. Conceptual hydrological approach to a geologically complex basin with scarce data: the Hula Valley. *Middle East Hydrogeol. J.* 28 (5), 1–20.
- Bar-Matthews, M., Ayalon, A., 1997. Late Quaternary paleoclimate in the Eastern Mediterranean region from stable isotope analysis of speleothems at Soreq Cave, Israel. *Quat. Res.* 47, 155–168.
- Bar-Matthews, M., Ayalon, A., Matthews, A., Sass, E., Halicz, L., 1996. Carbon and oxygen isotope study of the active water-carbonate system in a karstic Mediterranean cave: implications for paleoclimate research in semiarid regions. *Geochim. Cosmochim. Acta* 60 (2), 337–347.
- Bar-Matthews, M., Ayalon, A., Kaufman, A., 2000. Timing and hydrological conditions of sapropel events in the Eastern Mediterranean, as evident from speleothems, Soreq cave, Israel. *Chem. Geol.* 169, 145–156.
- Bar-Matthews, M., Ayalon, A., Gilmore, M., Matthews, A., Hawkesworth, C.J., 2003. Sea-land oxygen isotopic relationships from planktonic Foraminifera and speleothems in the Eastern Mediterranean region and their implication for paleorainfall during interglacial intervals. *Geochim. Cosmochim. Acta* 67 (17), 3181–3199.
- Bar-Matthews, M., Keinan, J., Ayalon, A., 2019. Hydro-climate research of the late Quaternary of the Eastern Mediterranean-Levant region based on speleothems research—A review. *Quat. Sci. Rev.* 221, 85–95.
- Bar-Yosef, O., Belfer-Cohen, A., 1989. The origins of sedentism and farming communities in the Levant. *J. World PreHistory* 3 (4), 447–499.
- Barker, S., Knorr, G., 2021. Millennial scale feedbacks determine the shape and rapidity of glacial termination. *Nat. Commun.* 12, 2273.
- Bartov, Y., Goldstein, S.L., Stein, M., Enzel, Y., 2003. Catastrophic arid episodes in the Eastern Mediterranean linked with the North Atlantic Heinrich events. *Geol.* 31 (5), 439–442.
- Baruch, U., Bottema, S., 1991. Palynological evidence for climatic changes in the levant ca. 17,000–9,000 BP. In: Bar-Yosef, O., Valla, F.R. (Eds.), *The Natufian Culture in the Levant*. International Monographs in Prehistory, Ann Arbor, Michigan, pp. 11–20. Archeological Series 1.
- Belfer-Cohen, A., Bar-Yosef, O., 2000. Early sedentism in the Levant: a bumpy ride to village life. In: Kuijt, I. (Ed.), *Life in Neolithic Farming Communities: Social Organization, Identity, and Differentiation*. Kluwer Academic Publishers, pp. 19–37.
- Belfer-Cohen, A., Goring-Morris, N., 2020. From the Epipaleolithic into the earliest Neolithic (PPNA) in the Southern Levant. *Documenta Praehist.* 47, 36–52.
- Belfer-Cohen, A., Hovers, E., 2005. The ground stone assemblages of the Natufian and Neolithic societies in the Levant—A brief review. *J. Isr. Prehist. Soc.* 35, 299–308.
- Belitzky, S., 2002. The structure and morphotectonics of the Gesher Benot Ya'aqov Area, Northern Dead Sea Rift, Israel. *Quat. Res.* 58, 372–380.
- Bemis, B.E., Spero, H.J., Bijma, J., Lea, D.W., 1998. Reevaluation of the oxygen isotopic composition of planktonic foraminifera: Experimental results and revised paleotemperature equations. *Paleoceanography* 13 (2), 150–160.
- Ben Dor, Y., Marra, F., Armon, M., Enzel, Y., Brauer, A., Schwab, M., Morin, E., 2021. Hydroclimatic variability of opposing late Pleistocene climates in the Levant revealed by deep Dead Sea sediments. *Clim. Past* 17 (6), 2653–2677.
- Binford, L.R., 1968. Post-Pleistocene adaptations. In: Binford, S., Binford, L.R. (Eds.), *New perspectives in archeology*, pp. 313–341. Aldine, Chicago.
- Björgvinsson, I., 2017. *Mollusc Taxa and Shell Preservation of the Early and Middle Epipaleolithic Archaeological Site Jordan River Dureijat in Israel*. Bachelor's thesis, University of Iceland.
- Bocquentin, F., Khalaily, H., Bar-Yosef Mayer, D.E., Berna, F., Biton, R., Boness, D., Dubreuil, L., Emery-Barbier, A., Greenberg, H., Goren, Y., Horwitz, L.K., Le Dosseur, G., Lernau, O., Mienis, H.K., Valentini, B., Samuelian, N., 2014. Renewed Excavations at Beisamoun: investigating the 7th millennium cal. BC of the Southern Levant. *J. Israel Prehist. Soc.* 44, 5–100.
- Bronk Ramsey, C., 2008. Deposition models for chronological records. *Quat. Sci. Rev.* 27 (1–2), 42–60.
- Buizert, C., Keisling, B.A., Box, J.E., He, F., Carlson, A.E., Sinclair, G., DeConto, R.M., 2018. Greenland-wide seasonal temperature during the last deglaciation. *Geophys. Res. Lett.* 45, 1905–1914.
- Bunin, E., Zhang, C., Sharon, G., Mischke, S., 2023. Physical, geochemical and chronostratigraphic data for sediments from the Jordan River Dureijat archeological site (Hula Valley, Israel). PANGAEA. <https://doi.org/10.1594/PANGAEA.959544> [dataset].
- Bunin, E., Zhang, C., Sharon, G., Mischke, S., 2024. Sedimentology and stratigraphy of the Jordan River Dureijat archeological site reveal subtle late Pleistocene water-level changes at Lake Hula, Jordan Valley, Israel. *J. Paleolimnol.* 71, 19–43.
- Camuera, J., Jiménez-Moreno, G., Ramos-Román, M.J., García-Alix, A., Jiménez-Espejo, F.J., Toney, L.J., Anderson, R.S., 2021. Chronological control and centennial-scale climatic subdivisions of the Last Glacial Termination in the western Mediterranean region. *Quat. Sci. Rev.* 255, 106814.
- Chen, C., Litt, T., 2018. Dead Sea pollen provides new insights into the paleoenvironment of the southern Levant during MIS 6–5. *Quat. Sci. Rev.* 188, 15–27.
- Cheng, H., Sinha, A., Verheyden, S., Nader, F.H., Li, X.L., Zhang, P.Z., Yin, J.J., Yi, L., Peng, Y.B., Rao, Z.G., Ning, Y.F., Edwards, R.L., 2015. The climate variability in northern Levant over the last 20,000 years. *Geophys. Res. Lett.* 42 (20), 8641–8650.
- Clark, P.U., Shakun, J.D., Baker, P.C., Bartlein, P.J., Brewer, S., Brook, E., Carlson, A.E., Cheng, H., Kaufman, D.S., Liu, Z., Marchitto, T.M., Mix, A.C., Morrill, C., Otto-Biesner, B.L., Pahnke, K., Russell, J.M., Whitlock, C., Adkins, J.F., Blois, J.L., Clark, J., Colman, S.M., Curry, W.B., Flower, B.P., He, F., Johnson, T.C., Lynch-Stieglitz, J., Markgraf, V., McManus, J., Mitrovica, J.X., Moreno, P.I., Williams, J.W., 2012. Global climate evolution during the last deglaciation. *Proc. Natl. Acad. Sci. USA* 109 (19), E1134–E1142.
- Cohen-Shacham, E., Dayan, T., Feitelson, E., de Groot, R.S., 2011. Ecosystem service trade-offs in wetland management: drainage and rehabilitation of the Hula, Israel. *Hydrolog. Sci. J.* 56 (8), 1582–1601.
- Columbu, A., Spötl, C., Fohlmeister, J., Hu, H.-M., Chiarini, V., Hellstrom, J., Cheng, H., Shen, C.-C., Waelde, J.D., 2022. Central Mediterranean rainfall varied with high northern latitude temperatures during the last deglaciation. *Comm. Earth. Env.* 3, 181.
- Cornuault, M., Vidal, L., Tachikawa, K., Licari, L., Rouaud, G., Sonzogni, C., Revel, M., 2016. Deep water circulation within the eastern Mediterranean Sea over the last 95 kyr: new insights from stable isotopes and benthic foraminiferal assemblages. *Palaeogeogr. Palaeoclimatol. Palaeoecol.* 459 (2016), 1–14.
- Cowgill, U., 1969. The Waters of Merom: a study of Lake Huleh I: introduction and general stratigraphy of a 54 m core. *Arch. Hydrobiol.* 66 (3), 249–272.
- Craig, H., 1961. Isotopic variations in meteoric waters. *Science* 133 (3465), 1702–1703.
- Craig, H., Gordon, L.I., 1965. Deuterium and Oxygen 18 variations in the ocean and the marine atmosphere. Stable Isotopes in Oceanographic Studies and Paleotemperatures. Spoleto, Italy, p. 122.
- Dafny, E., Burg, A., Gvirtzman, H., 2006. Deduction of groundwater flow regime in a basaltic aquifer using geochemical and isotopic data: the Golan Heights, Israel case study. *J. of Hydrol.* 330, 506–524.
- Dansgaard, W., 1964. Stable isotopes in precipitation. *Tellus* 16, 436–468.
- Dansgaard, W., Clausen, H.B., Gundestrup, N., Hammer, C.U., Johnsen, S.F., Kristinsdottir, P.M., Reeh, N., 1982. A new Greenland deep ice core. *Science* 218 (4579), 1273–1277.
- Denton, G.H., Alley, R.B., Comer, G.C., Broecker, W.S., 2005. The role of seasonality in abrupt climate change. *Quat. Sci. Rev.* 24, 1159–1182.
- Denton, G.H., Anderson, R.F., Toggweiler, J.R., Edwards, R.L., Schaefer, J.M., Putnam, A. E., 2010. The last glacial termination. *Science* 328, 1652–1656.

- Develle, A.-L., Herreros, J., Vidal, L., Sursock, A., Gasse, F., 2010. Controlling factors on a paleo-lake oxygen isotope record (Yammoúneh, Lebanon) since the last Glacial Maximum. *Quat. Sci. Rev.* 29, 865–886.
- Dimentman, C., Bromley, H.J., Por, F.D., 1992. Lake Hula: reconstruction of the fauna and hydrobiology of lost Lake. The Israeli Academy of Sciences and Humanities, Jerusalem, p. 170.
- Drummond, C.N., Patterson, W.P., Walker, J.C.G., 1995. Climatic forcing of carbon-oxygen isotopic covariance in temperate-region marl lakes. *Geology* 23 (11), 1031–1034.
- Dubreuil, L., Nadel, D., 2015. The development of plant food processing in the Levant: insights from use-wear analysis of Early Epipaleolithic ground stone tools. *Philos. Trans. R. Soc. Lond. B Biol. Sci.* 370, 20140357.
- Enzel, Y., Amit, R., Dayan, U., Crouvi, O., Kahana, R., Ziv, B., Sharon, D., 2008. The climatic and physiographic controls of the eastern Mediterranean over the late Pleistocene climates in the southern Levant and its neighboring deserts. *Global Planet. Change* 60, 165–192.
- Essallami, L., Sicre, M.A., Kallel, N., Labeyrie, L., Siani, G., 2007. Hydrological changes in the Mediterranean Sea over the last 30,000 years. *G-cubed* 8 (7), Q07002.
- Finlayson, B., Warren, G., 2010. Changing Natures: Hunter-Gatherers, First Farmers and the Modern World. Duckworth, Cambridge, p. 144.
- Flannery, K.V., 1969. Origin and ecological effects of early domestication in Iran and the Near East. In: Ucko, P.J., Dimbleby, G.W. (Eds.), *The domestication and exploitation of plants and animals*, pp. 73–100. Aldine, Chicago.
- Fleischer, E., 1968. The Subsurface Geology of the Hula Valley and Korazim Area. Geological Survey, Israel unpublished report.
- Fontes, J-Ch., Gonfiantini, R., Roche, M.-A., 1970. Deuterium and Oxygen-18 in Water of Lake Chad, pp. 387–402. IAEA-SM-129/23.
- Frumkin, A., Ford, D.C., Schwarzc, H.P., 2000. Paleoclimate and vegetation of the last glacial cycles in Jerusalem from a speleothem record. *Glob. Biogeochem. Cycles* 14 (3), 863–870.
- Gagin, A., Neumann, J., 1974. Rain stimulation and cloud physics in Israel. In: Hess, W. N. (Ed.), *Weather and Climate Modification*. John Wiley & Sons, pp. 454–494.
- Gat, J.R., Carmi, I., 1970. Evolution of the isotopic composition of atmospheric waters in the Mediterranean Sea area. *J. Geophys. Res.* 75 (15), 3039–3048.
- Gat, J.R., Carmi, I., 1987. Effect of climate changes on the precipitation patterns and isotopic composition of water in a climate transition zone: case of the Eastern Mediterranean Sea area. In: Solomon, S.I., Hogg, M.B.W. (Eds.), *Proceedings of the Vancouver Symposium: the Influence of Climate Change and Climate Variability on the Hydrologic Regime and Water Resources*, IAHS Proceedings and Reports, p. 168.
- Gat, J.R., Dansgaard, W., 1972. Stable isotope survey of the fresh water occurrences in Israel and the Jordan Rift Valley. *J. Hydrol.* 16, 177–211.
- Gat, J.R., Magaritz, M., 1980. Climatic variations in the Eastern Mediterranean Sea area. *Naturwissenschaften* 67, 80–87.
- Goldreich, Y., 2003. *The Climate of Israel: Observation, Research and Application*. Springer, Boston, p. 270.
- Goldsmith, Y., Polissar, P.J., Ayalon, A., Bar-Matthews, M., deMenocal, P.B., Broecker, W.S., 2017. The modern and last Glacial Maximum hydrological cycles of the Eastern Mediterranean and the Levant from a water isotope perspective. *Earth Planet Sci. Lett.* 457, 302–312.
- Goodfriend, G.A., Magaritz, M., 1988. Palaeosols and late Pleistocene rainfall fluctuations in the Negev Desert. *Nature* 332 (10), 144–146.
- Goring-Morris, N., 2009. Two Kebaran occupations near Nahal Soreq and the reconstruction of group ranges in the Early Epipaleolithic of the Israeli littoral. *Eurasian Prehistory* 6 (1–2), 75–93.
- Grant, K.M., Rohling, E.J., Bar-Matthews, M., Ayalon, A., Medina-Elizalde, M., Bronk Ramsey, C., Satow, C., Roberts, A.P., 2012. Rapid coupling between ice volume and polar temperature over the past 150,000 years. *Nature* 491, 477.
- Grant, K.M., Grimm, R., Mikolajewicz, U., Marino, G., Ziegler, M., Rohling, E.J., 2016. The timing of Mediterranean sapropel deposition relative to insolation, sea-level and African monsoon changes. *Quat. Sci. Rev.* 140 (15), 125–141.
- Groote, P.M., Stuiver, M., 1997. Oxygen 18/16 variability in Greenland snow and ice with 10^{-3} to 10^{-5} time resolution. *J. Geophys. Res.* 102 (C12), 26455–26470.
- Grosman, L., 2013. The Natufian chronological scheme – new insights and their implications. In: Bar-Yosef, O., Valla, F. (Eds.), *Natufian Foragers in the Levant. International Monographs in Prehistory*, pp. 622–635. Ann Arbor (USA).
- Hambright, K.D., Zohary, T., 1998. Lake Hula and Agmon: destruction and creation of wetland ecosystems in northern Israel. *Wetl. Ecol. Manag.* 6 (2), 83–89.
- Hammer, Ø., Harper, D.A.T., Ryan, P.D., 2001. PAST: paleontological statistics software package for education and data analysis. *Paleontologica Electronica* 4 (1), 4.
- Hazan, N., Stein, M., Agnon, A., Marco, S., Nadel, D., Negendank, J.F.W., Schwab, M.J., Neev, D., 2005. The late Quaternary limnological history of Lake Kinneret (Sea of Galilee), Israel. *Quat. Res* 63, 60–77.
- Heimann, A., 1990. The development of the Dead Sea Rift and its margins in northern Israel during the Pliocene and the Pleistocene. *Geological Survey of Israel Report GSI/28/90*, 1–83.
- Heimann, A., Ron, H., 1987. Young faults in the Hula pull-apart basin, central Dead Sea Transform. *Tectonophysics* 141 (1–3), 117–124.
- Heimann, A., Zilberman, E., Amit, R., Frieslander, U., 2009. Northward migration of the southern diagonal fault of the Hula pull-apart basin, Dead Sea Transform, northern Israel. *Tectonophysics* 476, 496–511.
- Hennekam, R., Jilbert, T., Schnetger, B., de Lange, G.J., 2014. Solar forcing of Nile discharge and sapropel S1 formation in the early to middle Holocene eastern Mediterranean. *Paleoceanogr. Paleoclimatol.* 29 (5), 343–356.
- Holmes, J., Chivas, A., 2002. Ostracod shell Chemistry—Overview. In: Holmes, J., Chivas, A. (Eds.), *The Ostracoda: Applications in Quaternary Research*, vol. 131. American Geophysical Union Geophysical Monograph Series, Washington DC, pp. 185–204.
- Horowitz, A., 1973. Development of the hula Basin, Israel. *Isr. J. Earth Sci.* 22, 107–139.
- Horowitz, A., Gat, J.R., 1984. Floral and isotopic indications for possible summer rains in Israel during wetter climates. *Pollen Spores* 26 (1), 61–68.
- Huang, J., Wan, S., Li, A., Li, T., 2019. Two-phase structure of tropical hydroclimate during Heinrich Stadial 1 and its global implications. *Quat. Sci. Rev.* 222, 105900.
- Hussein, M.A., Obuid-Allah, A.H., Mahmoud, A.A., Fangary, H.M., 2004. Ecology of eight species of freshwater ostracods (Crustacea) from Qena Governorate, Upper Egypt. *Egypt J Aquat Biol & Fish* 8 (4), 107–122.
- Incarbona, A., Marino, G., Di Stefano, E., Grelaud, M., Pelosi, N., Rodríguez-Sanz, L., Rohling, E.J., 2022. Middle-Late Pleistocene Eastern Mediterranean nutricline depth and coccolith preservation linked to Monsoon activity and Atlantic Meridional Overturning Circulation. *Global Planet. Change* 217, 103946.
- Israeli Meteorological Service, 2025. https://ims.gov.il/en/data_gov.
- Jara-Muñoz, J., Agnon, A., Fohlmeister, J., Tomás, S., Mey, J., Frank, N., Schroeder, B., Schroeder-Ritzrau, A., Garcin, Y., Darvasi, Y., Melnick, D., Mutti, M., Strecker, M.R., 2024. Unveiling the transition from paleolake Lisan to Dead Sea through the analysis of lake paleoshorelines and radiometric dating of fossil stromatolites. *G-cubed* 25, e2024GC011541.
- Johnsen, S.J., Clausen, H.B., Dansgaard, W., Fuhrer, K., Gundestrup, N., Hammer, C.U., Iversen, P., Jouzel, J., Stauffer, B., Steffensen, J.P., 1992. Irregular glacial interstadials recorded in a new Greenland ice core. *Nature* 359 (6393), 311–313.
- Jones, R.F., 1940. Report of the Percy Sladen Expedition to Lake Huleh: a contribution to the study of the fresh waters of Palestine: the plant ecology of the district. *J. Ecol.* 28 (2), 357–376.
- Kafri, U., Lang, B., 1987. New data on the Late Quaternary fill of the Hula Basin, Israel. *Isr. J. Earth Sci.* 36, 73–81.
- Kaufman, D., 1992. Hunter-gatherers of the Levantine Epipaleolithic: the sociological origins of sedentism. *J. Mediterr. Archaeol.* 5, 165–201.
- Kelts, K., Talbot, M., 1990. Lacustrine carbonates as geochemical archives environmental change and biotic/abiotic interactions. In: Tilzer, M.M., Serruya, C. (Eds.), *Large Lakes: Ecological Structure and Function*. Springer-Verlag, Berlin-Heidelberg, pp. 288–315.
- Kolodny, Y., Stein, M., Machlus, M., 2005. Sea–rain–lake relation in the last Glacial East Mediterranean revealed by $\delta^{18}\text{O}$ – $\delta^{13}\text{C}$ in Lake Lisan aragonites. *Geochem. Cosmochim. Acta* 69, 4045–4060.
- Kushnir, Y., Dayan, U., Ziv, B., Morin, E., Enzel, Y., 2017. Climate of the Levant: phenomena and mechanisms. In: Enzel, Y., Bar-Yosef, O. (Eds.), *Quaternary of the Levant: Environments, Climate Change, and Humans*. Cambridge University Press, Cambridge, pp. 31–44.
- Labuhn, I., Tell, F., von Grafenstein, U., Hammarlund, D., Kuhnhert, H., Minster, B., 2022. A modern snapshot of the isotopic composition of lacustrine biogenic carbonates – records of seasonal water temperature variability. *Biogeosciences* 19, 2759–2777.
- Landaïs, A., Capron, E., Masson-Delmotte, V., Toucanne, S., Rhodes, R., Popp, T., Vinther, B., Minster, B., Prié, F., 2018. Ice core evidence for decoupling between midlatitude atmospheric water cycle and Greenland temperature during the last deglaciation. *Clim. Past* 14, 1405–1415.
- Langgut, D., Almogi-Labin, A., Bar-Matthews, M., Weinstein-Evron, M., 2011. Vegetation and climate changes in the South Eastern Mediterranean during the last Glacial-Interglacial cycle (86 ka): new marine pollen record. *Quat. Sci. Rev.* 30, 3960–3972.
- Langgut, D., Cheddadi, R., Sharon, G., 2021. Climate and environmental reconstruction of the Epipaleolithic Mediterranean Levant (22.0–11.9 ka cal. BP). *Quat. Sci. Rev.* 270, 107170.
- Le Houede, S., Mojtabah, M., Bicchi, E., de Lange, G.J., Hennekam, R., 2020. Suborbital hydrological variability inferred from coupled benthic and planktic foraminiferal-based proxies in the southeastern Mediterranean during the last 19 ka. *Paleoceanogr. Paleoclimatol.* 35 (2), e2019PA003827.
- Leng, M., Marshall, J.D., 2004. Palaeoclimate interpretation of stable isotope data from lake sediment archives. *Quat. Sci. Rev.* 23, 811–831.
- Ludwig, P., Hochman, A., 2022. Last glacial maximum hydroclimate and cyclone characteristics in the Levant: a regional modeling perspective. *Environ. Res. Lett.* 17, 014053.
- Macdonald, D.A., Allentuck, A., Maher, L.A., 2018. Technological change and economy in the Epipaleolithic: Assessing the shift from Early to Middle Epipaleolithic at Kharan IV. *J. Field Archaeol.* 43 (6), 1–20.
- MacGregor, J., 1870. The Rob Roy on the Jordan: a Canoe Cruise in Palestine and Egypt, and the Waters of Damascus. John Murray, London.
- Maher, L., Richter, T., Stock, J.T., 2012. The Pre-Natufian Epipaleolithic: Long-term behavioral trends in the Levant. *Evol. Anthropol.* 21, 69–81.
- Marder, O., Biton, R., Boaretto, E., Feibel, C.S., Melamed, Y., Mienis, H.K., Rabinovich, R., Zohar, I., Sharon, G., 2015. Jordan River Dureijat – a new Epipaleolithic site in the Upper Jordan Valley. *J. Israel Prehist Soc.* 45, 5–30.
- Mariotti, A., 2010. Recent changes in the Mediterranean water cycle: a pathway toward long-term regional hydroclimatic change? *J. Clim.* 23 (6), 1513–1525.
- McGarry, S., Bar-Matthews, M., Matthews, A., Vaks, A., Schilman, B., Ayalon, A., 2004. Constraints on hydrological and paleotemperature variations in the Eastern Mediterranean region in the last 140 ka given by δD values of speleothem fluid inclusions. *Quat. Sci. Rev.* 23, 919–934.
- Meisch, C., 2000. *Freshwater Ostracoda of Western and Central Europe*. Spektrum, Heidelberg, Germany, p. 522.
- Menviel, L., Timmermann, A., Timm, O.E., Mouchet, A., 2011. Deconstructing the last glacial termination: the role of millennial and orbital-scale forcings. *Quat. Sci. Rev.* 30, 1155–1172.

- Miebach, A., Chen, C., Schwab, M., Stein, M., Litt, T., 2017. Vegetation and climate during the last Glacial high stand (ca. 28e22 ka BP) of the Sea of Galilee, northern Israel. *Quat. Sci. Rev.* 156, 47–56.
- Miebach, A., Stolzenberger, S., Wacker, L., Hence, A., Litt, T., 2019. A new Dead Sea pollen record reveals the last glacial paleoenvironment of the southern Levant. *Quat. Sci. Rev.* 214, 98–116.
- Milano, M., Ruellan, D., Fernandez, S., Dezetter, A., Fabre, J., Servat, E., 2012. Facing climatic and anthropogenic changes in the Mediterranean basin: what will be the medium-term impact on water stress? *C. R. Geosci.* 344, 432–440.
- Naughton, F., Sánchez Goñi, M.F., Kageyama, M., Bard, E., Duprat, J., Cortijo, E., Desprat, S., Malaizé, B., Joly, C., Rostek, F., Turon, J.-L., 2009. Wet to dry climatic trend in north-western Iberia within Heinrich events. *Earth Planet Sci. Lett.* 284, 329–342.
- Neumann, J., 1953. Energy balance of and evaporation from sweet water lakes of the Jordan Rift. *Bull. Res. Coun. Isr.* 2, 337–357.
- Olubanjo, O.A., Idowu, R.T., 2024. Evaluation of the distribution and abundance of ostracodes in Jabi Lake, Abuja, Nigeria. *Dir. Res. J. Public Health and Environ. Technol.* 9 (1), 53–60.
- Pedergnana, A., Cristiani, E., Munro, N., Valletta, F., Sharon, G., 2021. Early line and hook fishing at the epipaleolithic site of Jordan River Dureijat (Northern Israel). *PLoS One* 16 (10), e0257710.
- Rambeau, C.M.C., 2010. Palaeoenvironmental reconstruction in the Southern Levant: synthesis, challenges, recent developments and perspectives. *Phil. Trans. R. Soc. A* 368, 5225–5248.
- Rasmussen, S.O., Bigler, M., Blockley, S.P., Blunier, T., Buchardt, S.L., Clausen, H.B., Cvijanović, I., Dahl-Jensen, D., Johnsen, S.J., Fischer, H., Gkinis, V., Guillevic, M., Hoek, W.Z., Lowe, J.J., Pedro, J.B., Popp, T., Seierstad, I.K., Steffensen, J.P., Svensson, A.M., Vallelonga, P., Vinther, B.M., Walker, M.J.C., Wheatley, J.J., Winstrup, M., 2014. A stratigraphic framework for abrupt climatic changes during the last Glacial period based on three synchronized Greenland ice-core records: refining and extending the INTIMATE event stratigraphy. *Quat. Sci. Rev.* 106, 14–28.
- Reimer, P., Austin, W., Bard, E., Bayliss, A., Blackwell, P., Bronk Ramsey, C., Butzin, M., Cheng, H., Edwards, R., Friedrich, M., Grootes, P., Guilderson, T., Hajdas, I., Heaton, T., Hogg, A., Hughen, K., Kromer, B., Manning, S., Muscheler, R., Palmer, J., Pearson, C., van der Plicht, J., Reimer, R., Richards, D., Scott, E., Southon, J., Turney, C., Wacker, L., Adolphi, F., Buntgen, U., Capello, M., Fahrni, S., Fogtmann-Schultz, A., Friedrich, R., Kohler, P., Kudsk, S., Miyake, F., Olsen, J., Reinig, F., Sakamoto, M., Sookdeo, A., Talamo, S., 2020. The IntCal20 calibration curve (0–55 cal kBP). *Radiocarbon* 62, 725–757.
- Rice, A., Bunin, E., Plessen, B., Sharon, G., Mischke, S., 2023. Implications of sub-monthly oxygen and carbon isotope variations in Late Pleistocene *Melanopsis* shells for regional and local hydroclimate in the Upper Jordan River Valley. *Quat. Res.* 115, 146–159.
- Richter, T., Maher, L., 2013. Terminology, process and change: reflections on the Epipaleolithic of Southwest Asia. *Lевант* 45, 121–132.
- Rindsberger, M., Magaritz, M., Carmi, I., Gilad, D., 1983. The relation between air mass trajectories and the water isotope composition in the Mediterranean Sea. *Geophys. Res. Lett.* 10, 43–46.
- Rindsberger, M., Jaffe, S., Rahamim, S., Gat, J.R., 1990. Patterns of the isotopic composition of precipitation in time and space: data from the Israeli storm water collection program. *Tellus* 42B, 263–271.
- Roberts, N., Jones, M.D., Benkaddour, A., Eastwood, W.J., Filippi, M.L., Frogley, M.R., Lamb, H.F., Lneq, M.J., Reed, J.M., Stein, M., Stevens, L., Valero-Garcés, B., Zanchetta, G., 2008. Stable isotope records of Late Quaternary climate and hydrology from Mediterranean lakes: the ISOMED synthesis. *Quat. Sci. Rev.* 27, 2426–2441.
- Robinson, S.A., Black, S., Sellwood, B.W., Valdes, P., 2006. A review of palaeoclimates and palaeoenvironments in the Levant and Eastern Mediterranean from 25,000 to 5,000 years BP: setting the environmental background for the evolution of human civilization. *Quat. Sci. Rev.* 25, 1517–1541.
- Roskin, J., Porat, N., Tsoar, H., Blumberg, D.G., Zander, A.M., 2011. Age, origin and climatic controls on vegetated linear dunes in the northwestern Negev Desert (Israel). *Quat. Sci. Rev.* 30, 1649–1674.
- Rowe, P.J., Mason, J.E., Andrews, J.E., Marca, A.D., Thomas, L., van Calsteren, P., Jex, C. N., Vonhof, H.B., Al-Omari, S., 2012. Speleothem isotopic evidence of winter rainfall variability in northeast Turkey between 77 and 6 ka. *Quat. Sci. Rev.* 45, 60–72.
- Rozanski, K., Araguás-Araguás, L., Gonfiantini, R., 1993. Isotopic patterns in modern global precipitation. In: Swart, P.K., Lohmann, K.C., McKenzie, J., Savin, S. (Eds.), *Climate Change in Continental Isotopic Records*, vol. 78. American Geophysical Union, Washington DC, pp. 1–36. Geophysical Monograph Series.
- Rybakov, M., Fleischer, L., ten Brink, U., 2003. The Hula Valley subsurface structure inferred from gravity data. *Isr. J. Earth Sci.* 52 (3–4), 113–122.
- Seager, R., Liu, H., Henderson, N., Simpson, I., Kelley, C., Shaw, T., Kushnir, Y., Ting, M., 2014. Causes of increasing aridification of the Mediterranean region in response to rising greenhouse gases. *J. Clim.* 27 (12), 4655–4676.
- Seierstad, I.K., Abbott, P.M., Bigler, M., Blunier, T., Bourne, A., Brook, E., Buchardt, S.L., Buizert, C., Clausen, H.B., Cook, E., Dahl-Jensen, D., Davies, S., Guillevic, M., Johnsen, S.J., Pedersen, D.S., Popp, T.J., Rasmussen, S.O., Severinghaus, J., Svensson, A., Vinther, B.M., 2014. Consistently dated records from the Greenland GRIP, GISP2 and NGRIP ice cores for the past 104 ka reveal regional millennial-scale $\delta^{18}\text{O}$ gradients with possible Heinrich event imprint. *Quat. Sci. Rev.* 106, 29e46.
- Sharon, G., Feibel, C.S., Belitzky, S., Marder, O., Khalaily, H., Rabinovich, R., 2002. Jordan River Drainage Project damages Gesher Benot ya'aqv: a preliminary study of the archaeological and geological implications. In: Gal, Z. (Ed.), *Eretz Zafon—Studies in Galilean Archaeology*, pp. 1–19. Israel Antiquities Authority (Jerusalem), Jerusalem.
- Sharon, G., Barkai, R., Rosenberg, D., 2018. A man of his land: ammon Assaf (1928–2018). *J. Israel Prehist. Soc.* 48, 173–176.
- Sharon, G., Grosman, L., Allue, E., Barash, A., Bar-Yosef Mayer, D.E., Biton, R., Bunin, E., Langgut, D., Melamed, Y., Mischke, S., Valletta, F., Munro, N.D., 2020. Jordan River Dureijat: 10,000 years of intermittent epipaleolithic activity on the shore of Paleolake Hula. *PaleoAnthropology* 2020, 34–64.
- Shavit, A., Sharon, G., 2023. Can models of evolutionary transition clarify the debates over the Neolithic Revolution? *Philos. Trans. R. Soc. B* 378 (1872), 20210413.
- Stein, M., Starinsky, A., Katz, Goldstein SL, Machlus, M., Schramm, A., 1997. Strontium isotopic, chemical, and sedimentological evidence for the evolution of Lake Lisan and the Dead Sea. *Geochem. Cosmochim. Acta* 61 (18), 3975–3992.
- Stein, M., Goring-Morris, N., Ben Dor, Y., Erel, Y., 2025. Environmental setting of the Neolithic agricultural revolution across the fertile crescent. *Quat. Sci. Rev.* 355, 109265.
- Stiller, M., Hutchinson, G.E., 1980. The waters of Merom: a study of Lake Huleh VI. Stable isotopic composition of carbonates of a 54 m core, paleoclimatic and paleotrophic implications. *Arch. Hydrobiol.* 89, 275–302.
- Stockhecke, M., Timmermann, A., Kipfer, R., Haug, G.H., Kwiecien, Friedrich, T., Menviel, L., Litt, T., Pickarski, N., Anselmetti, F.S., 2016. Millennial to orbital-scale variations of drought intensity in the Eastern Mediterranean. *Quat. Sci. Rev.* 133, 77–95.
- Stuiver, M., 1970. Oxygen and carbon isotopic ratios of fresh-water carbonates as climatic indicators. *J. Geophys. Res.* 75 (27), 5247–5257.
- Survey of Israel, 1951. Israel 1:250,000 Map Series Sheet 1. Jerusalem.
- Talbot, M.R., 1990. A review of the palaeohydrological interpretation of carbon and oxygen isotopic ratios in primary lacustrine carbonates. *Chem. Geol.* 80, 261–279.
- Tchernov, E., 1992. The Levantine mammalian fauna – a short biogeographical review. *Isr. J. Zool.* 38 (3–4), 155–192.
- Thiede, J., 1978. A glacial mediterranean. *Nature* 276, 680–683.
- Tierney, J., Torfstein, A., Bhattacharya, T., 2022. Late Quaternary hydroclimate of the Levant: the leaf wax record from the Dead Sea. *Quat. Sci. Rev.* 289, 107613.
- Torfstein, A., Goldstein, S.L., Stein, M., Enzel, Y., 2013. Impacts of abrupt climate changes in the Levant from last Glacial Dead Sea levels. *Quat. Sci. Rev.* 69, 1–7.
- Torfstein, A., Goldstein, S.L., Kushnir, Y., Enzel, Y., Haug, G., Stein, M., 2015. Dead Sea drawdown and monsoonal impacts in the Levant during the last interglacial. *Earth Planet Sci. Lett.* 412, 235–244.
- Vadsaria, T., Zaragosi, S., Ramstein, G., Dutay, J.-C., Li, L., Siani, G., Revel, M., Obase, T., Abe-Ouchi, A., 2022. Freshwater influx to the Eastern Mediterranean Sea from the melting of the Fennoscandian ice sheet during the last deglaciation. *Sci. Rep.* 12, 8466.
- Vaks, A., Bar-Matthews, M., Ayalon, A., Matthews, A., Frumkin, A., Dayan, U., Halicz, L., Almogi-Labin, A., Schilman, B., 2006. Paleoclimate and location of the border between Mediterranean climate region and the Sahara-Arabian Desert as revealed by speleothems from the northern Negev Desert, Israel. *Earth Planet Sci. Lett.* 249, 384–399.
- Vaks, A., Bar-Matthews, M., Ayalon, A., Matthews, A., Matthes, A., Halicz, L., Frumkin, A., 2007. Desert speleothems reveal climatic window for African exodus of early modern humans. *Geol.* 35 (9), 831–834.
- Valdimarsson, B., 2017. Ostracod-Based Paleoenvironment Inferences for the Jordan River Dureijat Archaeological Site, Northern Israel. Bachelor's thesis, University of Iceland.
- Valla, F., Khalaily, H., Samuelian, N., Bocquentin, F., Bridault, A., Rabinovich, R., 2017. Eynan (Ain Mallaha). In: Enzel, Y., Bar-Yosef, O. (Eds.), *Quaternary of the Levant: Environments, Climate Change, and Humans*. Cambridge University Press, Cambridge, pp. 295–301.
- Valletta, F., Grosman, L., 2025. New insights into the pre-Natufian Epipaleolithic from the Ein Gev IV Nizzanan site (upper Jordan Valley). *Quat. Sci. Rev.* 356, 109294.
- Van Zeist, W., Baruch, U., Bottema, S., 2009. Holocene palaeoecology of the Hula area, northeastern Israel. In: Kaptijn, E., Petit, L.P. (Eds.), *A Timeless Vale: Archaeological and Related Essays on the Jordan Valley in Honour of Gerrit Van Der Kooij on the Occasion of his sixty-fifth Birthday*. Leiden University Press, Leiden, pp. 29–64.
- Von Grafenstein, U., Erlerkeuser, H., Trimborn, P., 1999. Oxygen and carbon isotopes in modern fresh-water ostracod valves: assessing vital offsets and autoecological effects of interest for palaeoclimate studies. *Palaeogeogr. Palaeoclimatol. Palaeoecol.* 148, 133–152.
- Washbourne, R., Jones, R.F., 1936. Percy Sladen expedition to Lake Huleh. *Nature* 137 (3473), 852–854.
- Weinberger, R., Gross, M.R., Sneh, A., 2009. Evolving deformation along a transform plate boundary: example from the Dead Sea Fault in northern Israel. *Tectonics* 28 (5), TC5005.
- Weinstein-Evron, M., 1983. The paleoecology of the Early Wurm in the Hula Basin, Israel. *Paleorient* 9 (1), 5–19.
- Wetzel, R.G., Likens, G.E., 2000. Lake Basin characteristics and morphometry. In: Wetzel, R.G., Likens, G.E. (Eds.), *Limnological Analyses*. Springer, New York, pp. 1–14.
- Wright, H.E., 1993. Environmental determinism in near eastern prehistory. *Curr. Anthropol.* 34 (4), 458–469.
- Xia, J., Ito, E., Engstrom, D.R., 1997. Geochemistry of ostracod calcite: part 1. An experimental determination of oxygen isotope fractionation. *Geochem. Cosmochim. Acta* 61 (2), 377–382.
- Zaarur, S., Affek, H., Stein, M., 2016. Last glacial-holocene temperatures and hydrology of the Sea of Galilee and Hula Valley from clumped isotopes in *Melanopsis* shells. *Geochem. Cosmochim. Acta* 179, 142–155.
- Zohar, I., Biton, R., 2011. Land, lake, and fish: investigation of fish remains from Gesher Benot Ya'aqv (paleo-Lake Hula). *J. Hum. Evol.* 60, 343–356.